STABLE ISOTOPE INVESTIGATION OF THE PRESENCE OF OCEAN ANOXIC EVENT 1D IN THE MENTELLE BASIN

By

HANNAH GHOTBI

Bachelor of Science in Geosciences

The University of Texas at Dallas

Richardson, Texas

2017

Submitted to the Faculty of the
Graduate College of the
Oklahoma State University
in partial fulfillment of
the requirements for
the Degree of
MASTER OF SCIENCE
Summer 2021

STABLE ISOTOPE INVESTIGATION OF THE

PRESENCE OF OCEAN ANOXIC EVENT 1D IN THE

MENTELLE BASIN

Thesis Approved:

Dr. Tracy Quan

Thesis Adviser

Dr. Natascha Riedinger

Dr. Michael Grammer

ACKNOWLEDGEMENTS

I would like to thank my friends and family and the many people who make up the faculty, staff, and graduate student population in the Boone Pickens School of Geology.

First, Dr. Tracy Quan for being real with me and supporting me throughout my learning process and pushing when I needed it, and most importantly, allowing me to pursue this degree. Dr. Tao Wu was instrumental in helping with all my lab work and making sure I was trained to use the EA-IRMS before his departure. Next are the wonderful and supportive members of my committee: Dr. Natascha Riedinger and Dr. Michael Grammer. Additionally, other faculty members who were attentive, taught me, and allowed me to talk to them were Dr. Ashley Burkett and Dr. Michelle Abshire. Dr. Ashley Burkett gets an extra special shout out because of how amazing she has made my last semester here. She assisted me with the basics concerning professional development and offered me a glimpse into her laboratory work and professional goals. She supported me in my efforts to finish the writing of the thesis.

I would like the thank all of the Expedition 369 scientists and the funding source for my research, USSSP Post-Expedition Award. I would like to thank William Andrews, Skylar Kaminski, Erin Merry, Dylan Morton, Amelia Kirkland, and Lauren Brown, who helped prepare the samples.

The first person in this school I was able to go to for basic questions on my research and about how things worked was Dr. Leye Adeboye. He helped me out with so many basics and throughout my graduate studies. He continued to give me good advice and made me feel welcome as a part of the lab group. He assisted me with my lab work, my proposal, my poster presentation, and this thesis.

I give thanks to all the other people who make up the Boone Pickens School of Geology who have personally helped me. There are too many to name, but there were many times we have all supported each other as we have gone through challenges in school and in life.

Name: HANNAH GHOTBI

Date of Degree: Summer 2021

Title of Study: STABLE ISOTOPE INVESTIGATION OF THE PRESENCE OF OCEAN ANOXIC EVENT 1D IN MENTLLE BASIN

Major Field: GEOLOGY

Abstract: Many studies investigating Ocean Anoxic Events (OAEs) used samples from areas that are around lower paleo latitudes typically in the Northern Hemisphere, mostly around the Atlantic Ocean and former Western Interior Seaway. OAE 1d (Albian-Cenomanian boundary) is suspected to be a global event, but paleoredox data from the Southern Hemisphere are limited. The samples used in this study were collected from two Holes, U1513C and U1516C, drilled in the Mentelle Basin off the southwest coast of Australia during International Ocean Discovery Program (IODP) Expedition 369.
For Hole U1513C, the redox state is variable. The stable nitrogen isotope values of acidified samples ($\delta^{15}N_{acidified}$) for U1513C range from -1.2 ‰ to 2.2 ‰. The $\delta^{15}N_{acidified}$ data suggest that an interval at Hole U1513C displays a trend of a possible OAE 1d occurrence with $\delta^{15}N_{acidified}$ values. The trend is more negative $\delta^{15}N_{acidified}$ values that are possibly anoxic, flanked by more positive $\delta^{15}N_{acidified}$ values indicate suboxic conditions. This hypothesized trend for $\delta^{15}N_{acidified}$ values for OAE 1d that if seen with other proxies such as $\delta^{13}C_{org}$ and TOC would confirm that OAE 1d occurred at this interval. At Hole U1516C, the data indicate that the redox state is not as variable as at Hole U1513C. For Hole U1516C, the change in $\delta^{15}N_{acidified}$ values is generally less than 1 ‰ and ranges from -1.2 to 0.6 ‰ The lack of change across this Hole and a large hiatus in a possible OAE 1d interval do not aid the interpretation of the $\delta^{15}N_{acidified}$ values. The redox state at this site could be oxic or anoxic due to low $\delta^{15}N_{acidified}$ values at this Hole, but oxic conditions are more likely, due to low organic matter concentrations. The area was influenced by rifting from the breakup of the Indian, Australian, and Antarctic plates. The depositional environment of the Mentelle Basin at the time of OAE 1d is a subsiding basin with a potential depth of 600 – 2000 meters with deposition of claystone indicating a low energy environment. The Mentelle Basin has been shown to have had restricted water circulation. All of these factors indicate possible anoxia could have occurred during OAE 1d. Without at least one other proxy such as $\delta^{13}C_{org}$, we cannot confidently constrain the redox state and cannot confirm OAE 1d's occurrences at either Hole. A much-needed addition to this study would be $\delta^{13}C_{org}$ and TOC measurements, as is common for OAE investigations.

TABLE OF CONTENTS

Chapter Page

I. INTRODUCTION 1

Study Location 6

II. REVIEW OF LITERATURE 10

Stable Carbon Isotopes Relating to OAE Studies 12
Stable Nitrogen Isotopes Relating to OAE Studies 15
Geologic Setting 19

III. METHODOLOGY 27

IV. RESULTS 33

V. DISCUSSION 40

Hole U1513C 40
Hole U1516C 41
General Discussion 42
Conclusion 44

REFERENCES 46

APPENDICES 50

LIST OF TABLES

Table Page

1 Definition of redox states using water column oxygen content.....15

LIST OF FIGURES

Figure Page

1 Time scale showing the stratigraphic position and nomenclature of OAEs 2
2 Conceptual model of a characteristic increase of $\delta^{13}C$ when OAE 1d occurs.....4
3 Conceptual model of how the $\delta^{15}N$ values will change with the redox state.....5
4 Location of Mentelle Basin A. Paleo and B. Current 7
5 Representation of large-scale ocean transgression during the Cretaceous 8
6 Global reconstruction of the mid-Cretaceous (Albian) period 11
7 Carbon proxy records from OAE 1d A. Italy and B. New Mexico 13
8 Marine nitrogen budget and processes affecting the distribution of nitrogen isotopes in the open ocean.....16
9 Conceptual data set construction for an OAE 1d occurrence 18
10 Reconstruction of SW. Australian Margin A. 108 Ma and B. 100 Ma.....21
11 Stratigraphic column for Site U1513 23
12. Stratigraphic column for Hole U1516C sections A. 38R, B. 39R, C. 40R.....24
13 Approximate age of Hole U1513C 28
14 Approximate age of Hole U1516C 29
15 A. How a δ ratio is calculated and B. How a $\delta^{15}N$ is calculated.....31
16 $\delta^{15}N_{acidified}$ profile for Hole U1513C 35
17 $\delta^{15}N_{acidified}$ profile for possible OAE 1d in Hole U1513C.....36
18 $\delta^{15}N_{acidified}$ profile Hole U1516C.....37
19 $\delta^{15}N_{acidified}$ profile for possible OAE 1d in Hole U1513C.....38

CHAPTER I

INTRODUCTION

The Cretaceous (145 - 66 Ma) was a period of greenhouse conditions and many oceanic anoxic events (OAEs) (Figure 1). During OAEs, anoxic conditions persisted throughout the world's oceans to varying degrees, resulting in the deposition of organic rich sediments. Furthermore, OAEs were regional to global in scale (Schlanger and Jenkyns, 1976). The exact causes for ocean anoxic events are debated, but most scholars agree that greenhouse conditions have been determined to be the main driver (Jenkyns et al., 2001; Giraud et al., 2003; Jenkyns, 2003; Jenkyns, 2010; Bottini and Erba, 2018). Some scholars postulate that the mid-Cretaceous was the start of a large rise in sea level which changed the ocean/climate system, because of increased oceanic crust production and degassing of greenhouse gasses (Schlanger and Jenknys, 1976; Jenkyns, 2003; Leckie et al., 2002; Scott et al., 2013). Other studies theorize that increased productivity occurred and was caused by mechanisms, such as intensified mixing of the water column (Petrizzo et al., 2008), or that there were increased upwelling zones (Wilson and Norris, 2001; Juniam and Arthur, 2007; Hay, 2008; Jenkyns, 2010). Past environments of a complex period, such as the Cretaceous, can be studied through many methods, including the construction of biostratigraphic columns, geochemical proxies, and biomarkers (Jenkyns, 2010, and references therein). The goal of this research project was to use stable nitrogen isotopes such as geochemical proxy to determine the paleoredox state of the selected sites, to determine if a selected OAE occurred in a selected basin.

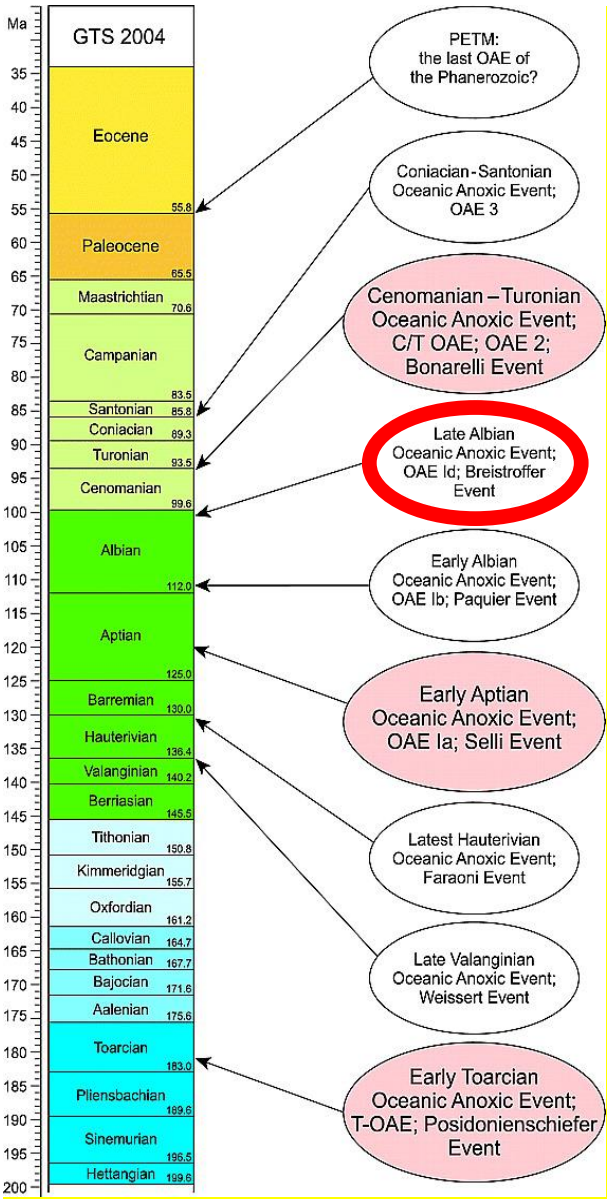

Figure 1. Time scale showing the stratigraphic position and nomenclature of Ocean Anoxic Events, modified from Jenkyns (2010). OAE 1d is outlined in red.

Geochemical proxies are used to determine paleoenvironmental factors by evaluating parameters, such as redox regime, or the state of preservation/productivity at the time sediments were deposited (Altabet and Francois, 1994; Scholle and Arthur, 1980; Jenkyns, 2010, and references within). A positive or negative excursion of $\delta^{13}C$ for both carbonate and organic carbon is the main identifier of OAEs (Scholle and Arthur, 1980). A change in $\delta^{13}C$ is interpreted as a change in burial and preservation of organic material enriched with either the lighter carbon isotope, ^{12}C, or the heavier isotope, ^{13}C (Scholle and Arthur, 1980; Hay, 2008; Jenkyns, 2010). For most OAEs, the positive $\delta^{13}C$ excursion that defines the event is caused by increased burial of sediments which preserved the isotopic signature of the heavier ^{13}C isotope (Scholle and Arthur, 1980; Wilson and Norris, 2001; Leckie et al., 2002; Scott at al., 2013; Bottini and Erba, 2018). This is because organisms preferentially take in the ^{12}C. If there is a depletion in the water column of the lighter carbon isotope, organisms will be forced to take in the heavier carbon isotope. Under these conditions, the organisms are enriched in ^{13}C. When these organisms die and are preserved, the sediments should reflect an enrichment in the heavier carbon isotope, ^{13}C of the organic matter (Leckie et al., 2002). Elevated TOC concentrations, compared to before and after the OAE, should occur almost concurrently with the positive excursion in $\delta^{13}C$ values during the OAE because the lack of oxygen in the water column allows for less degradation of organic matter. An excursion of $\delta^{13}C$, along with changing TOC values, has become the leading identifier of OAEs. A conceptual model for how $\delta^{13}C$ changes during an OAE is shown in Figure 2 (Scholle and Arthur, 1980; Jenkyns, 2010).

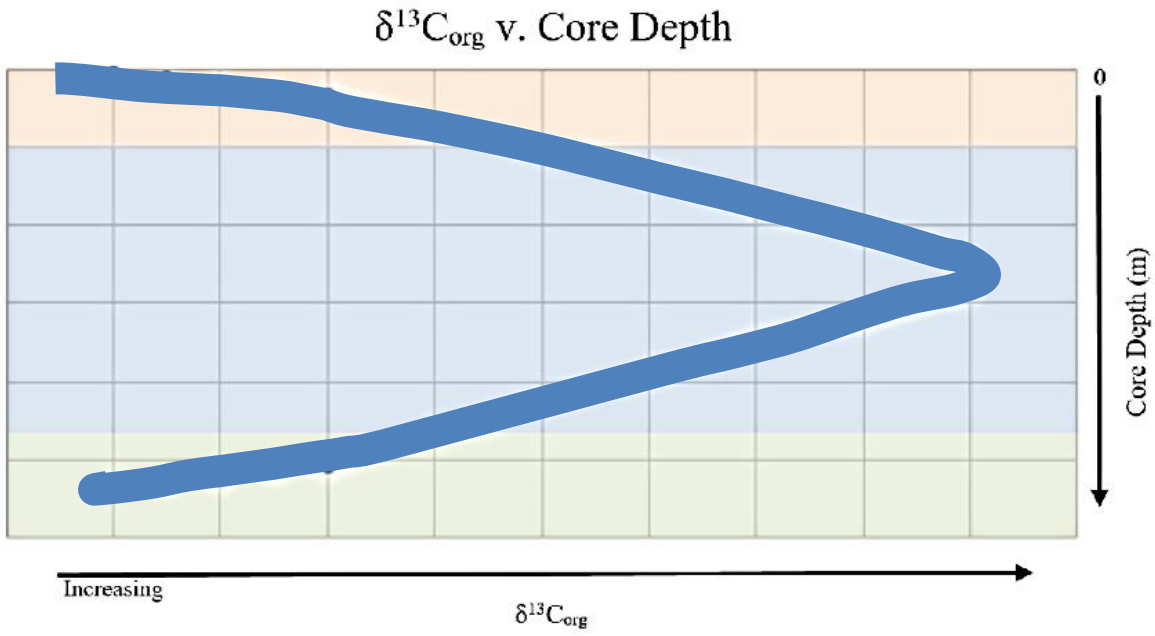

Figure 2. Conceptual model of a characteristic trend of $\delta^{13}C_{org}$ when an OAE occurs. The light green band is before the OAE, blue is during and orange is after. In the green area, the hypothetical water column is not in an anoxic state. This is why the $\delta^{13}C_{org}$ value is more positive in the blue area than in the green area. The blue area indicates the onset and duration of an OAE, so anoxic conditions would occur along with increased preservation of organic matter enriched in the heavier carbon isotope, C^{13}. The orange band shows a gradual decrease in $\delta^{13}C_{org}$ values and a return to pre OAE $\delta^{13}C_{org}$ values (Schlanger and Jenkyns, 1976; Scholle and Arthur, 1980; Leckie et al., 2002; Jenkyns, 2010 and references within).

As shown in Figure 3, the relative values for bulk sedimentary $\delta^{15}N$ data for oxic and anoxic environmental conditions in the water column are lower than for suboxia (Altabet and Francois, 1994; Quan et al., 2013b). Knowledge of the redox conditions through interpretation of a proxy, $\delta^{15}N$, can provide important information. If an OAE occurred at a location, anoxic conditions are expected to arise (Sigman and Casciotti, 2001; Quan et al., 2013a; Juniam and Arthur, 2018). This study aimed to determine if OAE 1d (Albian-Cenomanian boundary, Figure 1) occurred using $\delta^{13}C$ and $\delta^{15}N$ geochemical values and TOC. The $\delta^{13}C_{org}$ would show the increased

preservation and burial that would occur during anoxic conditions (Scholle and Arthur, 1980; Leckie et al., 2002; Jenkyns, 2010 and references therein) and the $\delta^{15}N_{acidified}$ values will show the change in redox regime (Rau et al., 1987; Jenkyns et al., 2001; Ohkouchi et al., 2006; Jenkyns et al., 2007; Juniam and Arthur, 2007).

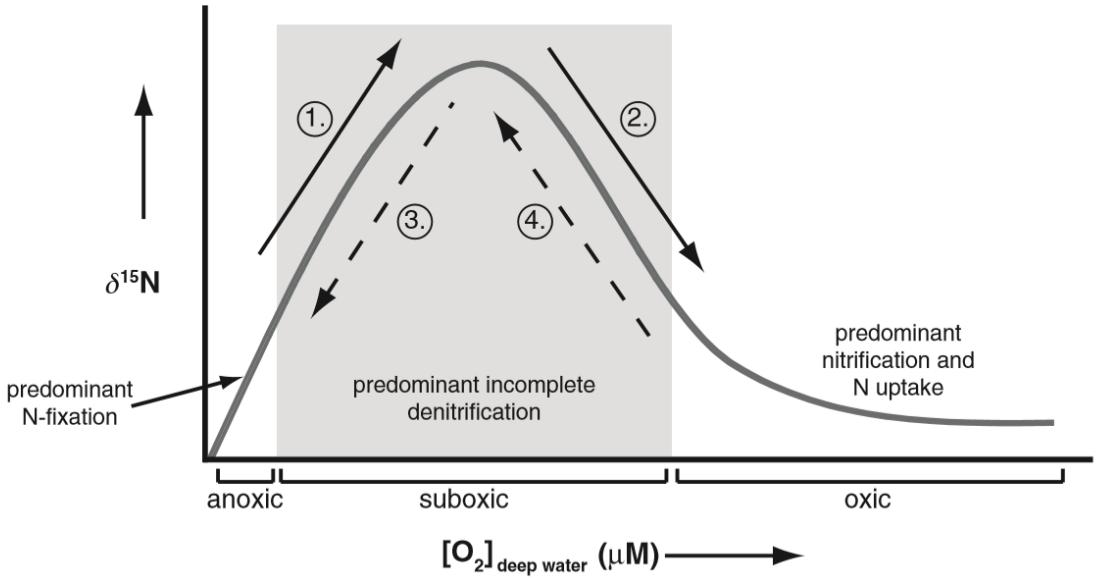

Figure 3. Conceptual model of how $\delta^{15}N$ sediment values will change with the redox state. The grey shaded area indicates suboxic conditions. The arrows show how the $\delta^{15}N$ value changes as oxygen content changes. The $\delta^{15}N$ values increase when suboxia is present, due to the fractionation resulting from denitrification during these conditions. The curve shows that the $\delta^{15}N$ value has a more positive value during suboxic events and a lower value during both anoxic and oxic events. (1.) Water column transitioning from anoxia to suboxia. (2.) Water column transitioning from suboxia to oxic. (3.) Water column transitioning out of suboxia to anoxia. (4.) Transition from oxic to suboxia (Quan et al., 2013b).

OAE 1d research has not focused on areas such as the southern hemisphere, as compared to the northern hemisphere, particularly in areas with restricted circulation. (Wilson and Norris, 2001; Scott at al., 2013; Bottini and Erba, 2018). The OAE that was examined in this research is OAE 1d, which occurred at the Albian-Cenomanian boundary in the mid-Cretaceous approximately 100 Ma (Petrizzo et al., 2008; Jenkyns, 2010; Scott et al., 2013; Bottini and Erba, 2018) (Figure 1). OAE 1d is not studied as much as other events such as OAE 2 or OAE 1a (Jenkyns, 2010 and references). Because of this, more studies at different study locations, including in the southern hemisphere, are needed to determine if the growing consensus that OAE 1d was a global event (Wilson and Norris, 2001; Jenkyns, 2010).

Study Location

The sediment samples that were used for this research project are from International Ocean Discovery Program (IODP) Expedition 369, and the interval from which these sentiments were taken was expected to contain OAE 1d. The samples were taken from the Mentelle Basin off the southwestern coast of Australia, as seen in Figure 4A, denoted by MB, and come from two Holes, U1513C and U1516C, as seen in Figure 4B, on the western side of the basin.

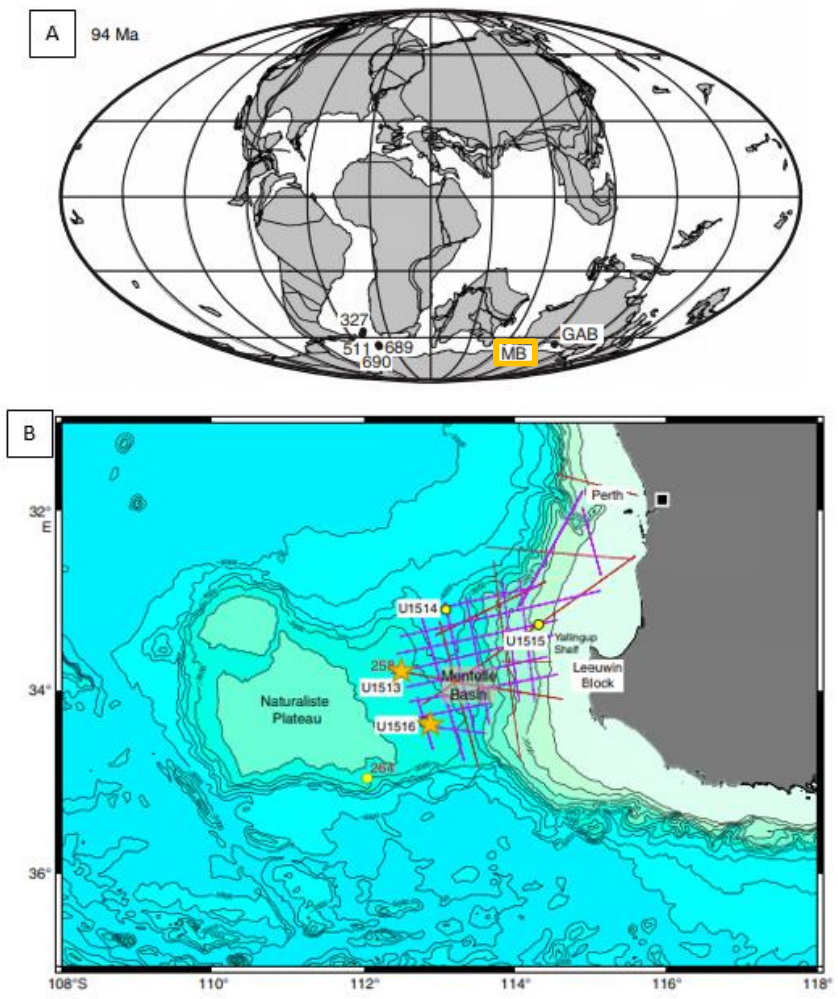

Figure 4. A. Location of Mentelle Basin (MB) around the time of Ocean Anoxic Event 1d. After Huber et al., (2018). B. Location of Sites in Mentelle Basin drilled by International Ocean Discovery Program (IODP) Exposition 369. Location of Holes U1513C and U1516C are indicated by yellow stars. After Huber et al., (2018).

The Cretaceous was a period of dynamic tectonic changes, with large transgressions that caused significant environmental shifts (Schlanger and Jenkyns, 1976; Hay, 2008). Around the time of OAE 1d, the start of a large transgression (seen in Figure 5) was caused by increased tectonic

activity. All of these events combined could have resulted in a change of water column redox conditions and productivity at the study location (Hay, 2008).

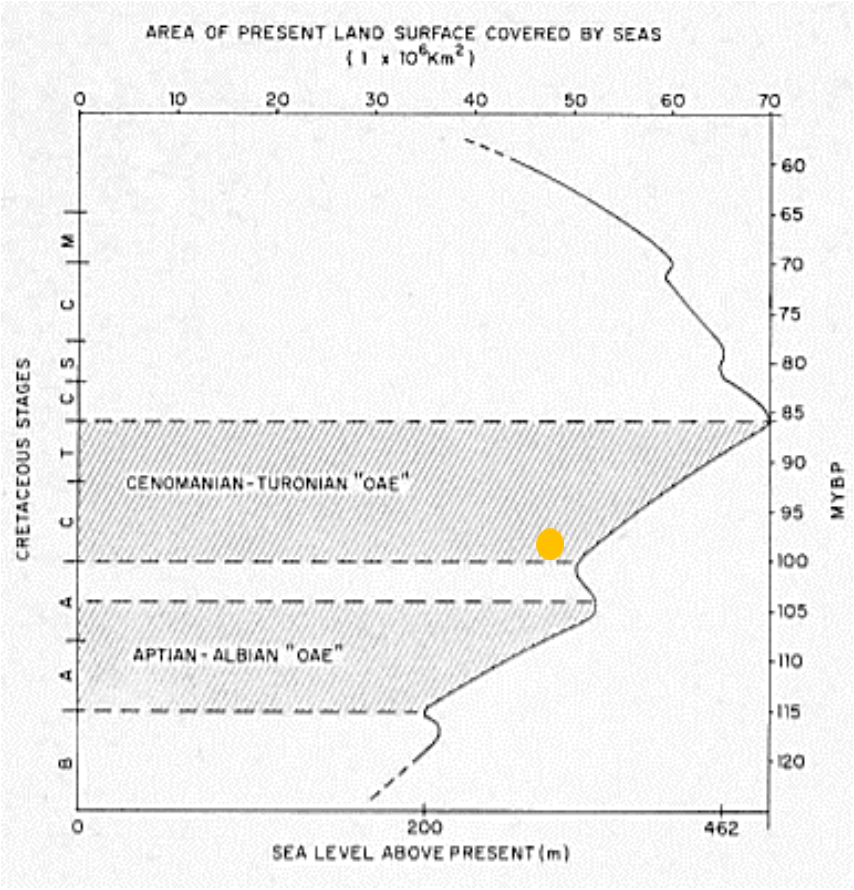

Figure 5. Representation of large-scale ocean transgression during the Cretaceous. Our target event, Ocean Anoxic Event 1d is represented by a yellow dot at the start of the second transgression (Schlanger and Jenkyns, 1976).

CHAPTER II

LITERATURE REVIEW

The increase in CO_2 and other carbon sources during the Cretaceous caused large scale perturbations of the carbon cycle, resulting in many OAEs (Leckie et al., 2002; Gallagher et al., 2005; Jenkyns, 2010). Even though many identified OAEs, including OAE 1d, show a positive stable carbon isotope ($\delta^{13}C$) excursion because of increased preservation and/or productivity through the events, not all will have this as the indication of the event (Jenkyns, 2010). OAEs that have negative $\delta^{13}C$ excursions, such as OAE 1a and the Early Toarcian OAE, are a result of releases of isotopically lighter carbon sinks, such as large-scale degassing of CO_2 from such events as venting from volcanogenic sources, thermal metamorphism of coals, and/or dissociation of gas hydrates (Jenkyns, 2010 and references within). The positive excursion of $\delta^{13}C$ for OAEs is mainly attributed to increased primary productivity through planktonic organisms, due to the fixation of isotopically lighter organic matter (Jenkyns, 2010 and references therein).

The conclusion made by Wilson and Norris, (2001) was that OAE 1d was a global event, because of the wide latitude range of sample locations that displayed similar carbon isotopic signatures, such as a positive excursion of $\delta^{13}C$ indicating the occurrence of OAE 1d at the study location. Before the work done by researchers such as Wilson and Norris, (2001), OAE 1d was thought to be regional, because the only occurrences of OAE 1d were in the Atlantic Ocean and western interior seaway. The focus of sampling in these areas shows that there is a bias that does not

include many higher latitude sites (Wilson and Norris, 2001), especially in the Southern Hemisphere (Figure 6). A reason for widespread anoxic conditions could be that during the

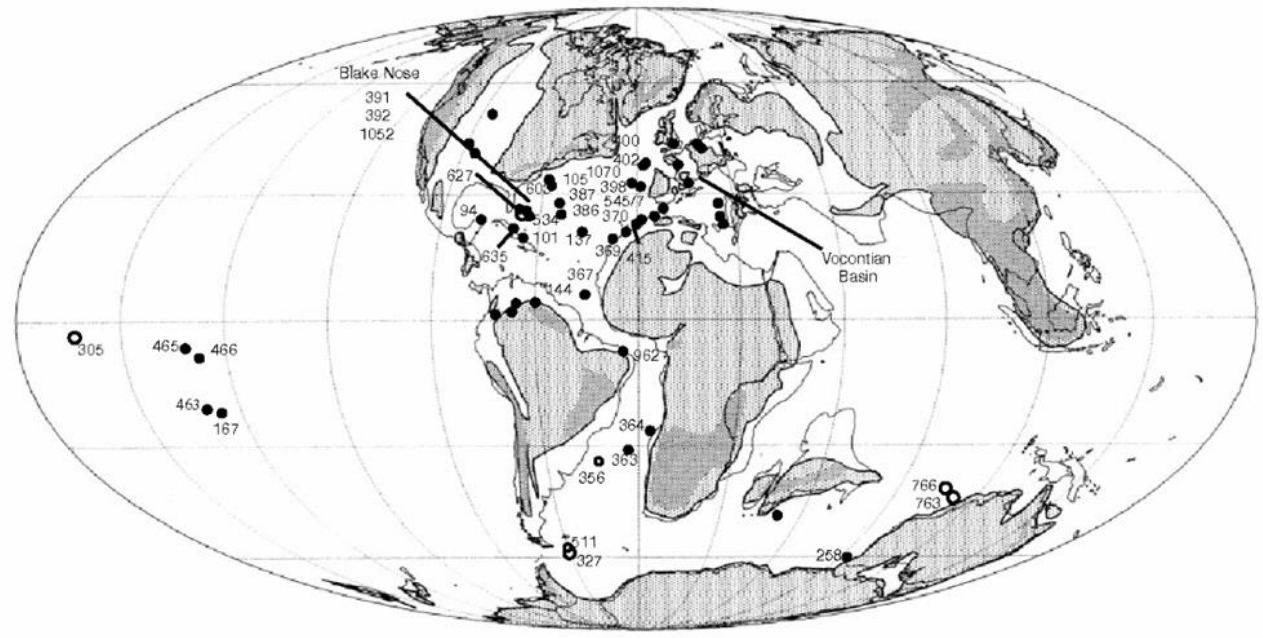

Figure 6. Reconstruction of the mid-Cretaceous (Albian) period showing the global location of sites with the well-dated sections correlative to OAE 1d. Sites, where OAE 1d was proven to occur, are denoted by the filled in circles (Wilson and Norris 2001).

Cretaceous, the proto-Atlantic Ocean was smaller and circulation was limited, which create conditions that are optimal for anoxia to occur (Schlanger and Jenkyns, 1976; Hay, 2008; Meyers and Kump, 2008; Jenkyns, 2010). This is because restriction of circulation and warmer climates is a combination that is ideal for anoxia to occur. If ocean circulation is restricted, anoxia is more likely to occur, because the input of more oxygenated waters decreases and the dissolved oxygen in the waters is used by organisms through respiration and the process of oxidizing organic matter. If more oxygenated waters are not flowing to an area more quickly than organisms are using the dissolved oxygen, the water column will become depleted in dissolved oxygen, shifting

from oxic to suboxic and/or anoxic water conditions (Karl and Michaels, 2001; Meyers and Kump, 2008; Quan et al., 2013a; Rivera et al., 2015). We can see in Figure 6 that the number of sites in the proto-Atlantic outnumbers other study sites in other areas of the world for OAE 1d (Rau et al., 1987; Jenkyns, 2001; Ohkouchi et al., 2006; Jenkyns et al., 2007; Juniam and Arthur, 2007; Petrizzo et al., 2008; Giraud et al., 2013; Scott et al., 2013; Bottini and Erba, 2018). There is a need to examine more sites that are outside of this area, to provide sufficient evidence of the global nature of this OAE.

Stable Carbon Isotopes Relating to OAE Studies

The geochemical proxy that is commonly used as an indicator of OAE occurrences is the $\delta^{13}C$ value, either carbonate or organic (Scott et al., 2013, Bottini and Erba, 2018). This is because the $\delta^{13}C$ value can be interpreted to indicate the level of preservation and burial of organic material (Scholle and Arthur, 1980; Jenkyns, 2010). The $\delta^{13}C$ value, carbonate or organic, is often coupled with TOC measurements, because more TOC will be preserved in the sediment if there is increased burial (Scholle and Arthur, 1980; Jenkyns, 2010; Scott et al., 2013). The $\delta^{13}C$ trend for OAE 1d is a positive excursion during the event, as seen in both studies in Figure 7. In Bottini and Erba, (2018), the researchers use $\delta^{13}C_{carb}$ as the stable carbon isotope proxy. This was done because the aim of their study was to test nannofossils as paleotemperature and paleoenvironmental indicators and their limitations in the Mid-Cretaceous. The use of $\delta^{13}C_{carb}$ is helpful when used with other proxies, such as nannofossils, to aid in the identification of events with specific chemostratigraphic signatures, such as OAEs, in areas where the traditional indicators, such as organic rich shale beds, are not as visible (Petrizzo et al., 2008; Bottini and

Erba, 2018). The researchers Bottini and Erba, (2018) wanted to focus on faunal turnover and the identification of OAEs, so the researchers used an inorganic $\delta^{13}C$ proxy. The $\delta^{13}C_{carb}$ and nannofossils occurrences showed that there was faunal turnover and changes in water fertility throughout the Cretaceous. The researchers concluded that these changes were caused by OAEs, including OAE 1d (Figure 7A), that can affect areas on a regional to global scale (Bottini and Erba, 2018). In Scott et al., (2013) the researchers also used inorganic $\delta^{13}C$ proxies, but used $\delta^{13}C_{org}$ to identify OAE 1d. The researchers in the study, as seen in Figure 7B, obtained $\delta^{13}C_{org}$ values before, during and after OAE 1d's occurrence and used the inorganic $\delta^{13}C$ proxies to estimate other factors such as post depositional diagenetic alteration. There was not a significant

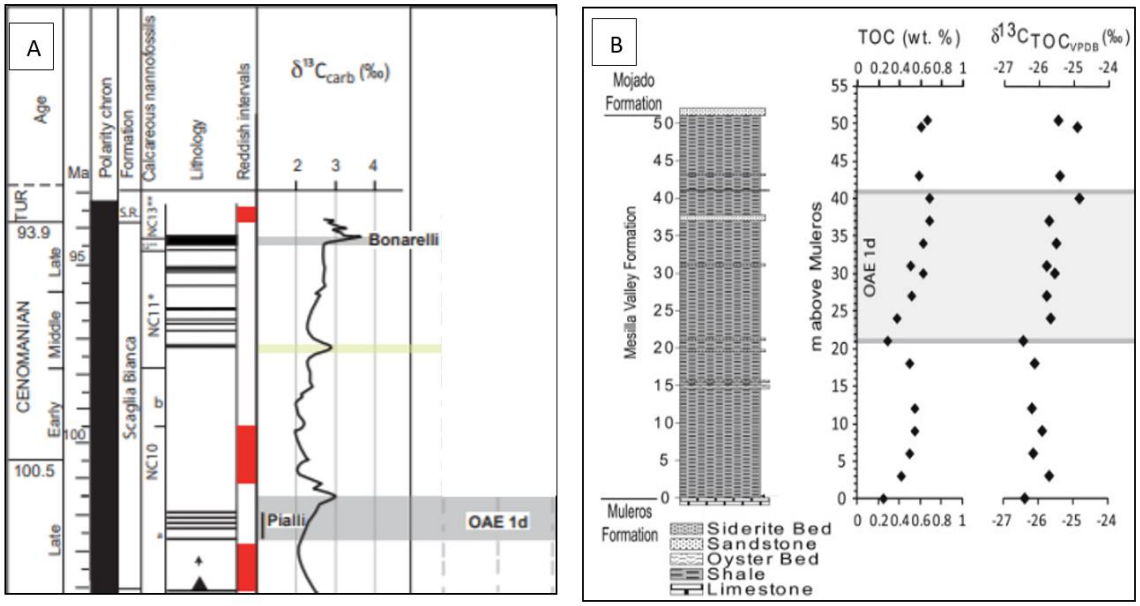

Figure 7. Stable carbon isotopes for OAE 1d occurrences taken from A) Italy (Bottini and Erba 2018); and B) New Mexico, USA (Scott et al., 2013).

amount of alteration seen and the positive $\delta^{13}C_{org}$ excursion during OAE 1d supports that conclusion (Scott et al., 2013). There is a positive excursion in both study areas in Figure 7 during

the event, with values that are more negative before and after the event. The magnitude of the change in the $\delta^{13}C$ values in each study differs, but the same trend of a positive $\delta^{13}C$ excursion, (carbonate or organic), during OAE 1d is seen at both study areas in Italy (Bottini and Erba, 2018) and New Mexico, USA (Scott et al., 2013).

The geochemical proxies $\delta^{13}C$ and TOC can also be used to indicate periods of high preservation and productivity (Scholle and Arthur, 1980; Leckie et al., 2002; Jenkyns, 2010 and references within). The application of $\delta^{13}C$ as a proxy is common when studying OAEs (Wilson and Norris, 2001; Petrizzo et al., 2008; Jenkyns, 2010; Scott et al., 2013; Bottini and Erba, 2018). The reason is because studies have shown that when more organic matter is deposited, the $\delta^{13}C$ (carbonate and organic) values becomes more positive relative to the values that occur before the OAE (Petrizzo et al., 2008; Jenkyns, 2010; Scott et al., 2013; Bottini and Erba, 2018). The values vary, but are usually within the range of -30‰ to -25‰ for $\delta^{13}C_{org}$ (Petrizzo et al., 2008; Jenkyns, 2010; Scott et al., 2013). During an OAE, more organic matter is deposited and preserved, because of the decreased amount of dissolved oxygen in the water column and increased productivity (Wilson and Norris, 2001; Leckie et al., 2002 Petrizzo et al., 2008; Scott et al., 2013; Bottini and Erba, 2018). An important aspect of using geochemical proxies, such as $\delta^{13}C$ (carbonate or organic) when studying OAEs, is to see a difference in values during the event compared to pre and post OAE data, as seen in Figure 7. Total organic carbon will show an increase in concentration that should correlate with the positive excursion in the $\delta^{13}C$ profiles. The TOC value in sediments will increase if the water column is anoxic. When there are anoxic water conditions, there is little to no oxygen in the water column. These conditions increase the

amount of organic matter that is not eaten by organisms or degraded by O_2 to the seafloor (Meyers and Kump, 2008; Quan et al., 2013b; Rivera et al., 2015).

Stable Nitrogen Isotopes Relating to OAE studies

Redox is used to describe how oxygenated the water column is by examining sediments. In this study, we are using $\delta^{15}N$ to determine the paleoredox state of selected sediments (Altabet and Francois, 1994; Sigman and Casciotti, 2001). The redox states in the water column are broadly referred to as anoxic, suboxic, and oxic. These redox states can be defined by water column oxygen content (ml O_2/l H_2O), as described by Tyson and Pearson, 1991 in Table 1.

Table 1. Definition of redox states using water column oxygen content (Tyson and Pearson, 1991).

Redox State	Water column oxygen content (ml O_2/l H_2O)
Oxic	> 2
Suboxic	0.2-2
Anoxic	< 0.2

Dissolved oxygen concentrations affect the nitrogen cycle and also indicate a redox state (Altabet and Francois, 1994; Karl and Michaels, 2001). Nitrogen cycling in a marine water column is primarily driven by microorganisms. These organisms that facilitate the different steps of the nitrogen cycle favor the lighter nitrogen isotope (^{14}N) over the heavier isotope (^{15}N). This fractionation is particularly strong for denitrification in the water column, as seen in Figure 8, resulting in organic matter that is incorporated into sediments with enriched values of the heavier

isotope, ^{15}N and higher $\delta^{15}N$ values during suboxic conditions (Figure 3) (Altabet and Francois, 1994; Sigman and Casciotti, 2001; Quan et al., 2013b; Rivera et al., 2015). The proxy $\delta^{15}N$ of sediments has been shown to accurately reflect the paleo redox state in the preserved sediments, because of how the nitrogen cycle changes with dissolved oxygen content in the water column (Altabet and Francois, 1994; Sigman and Casciotti, 2001; Quan et al., 2013a; Juniam and Arthur, 2018).

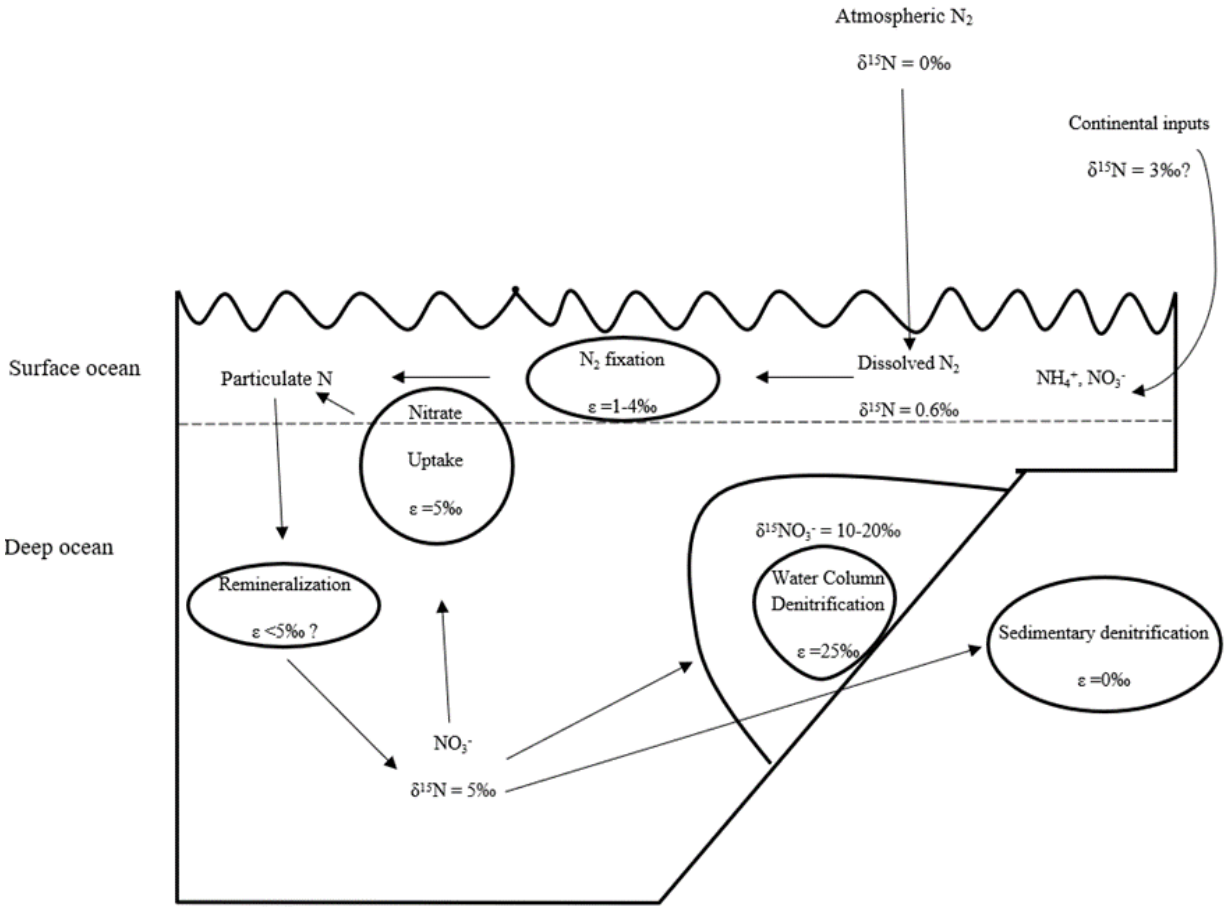

Figure 8. Marine nitrogen cycling in a water column with differentiation between surface and deep ocean areas. The ε value is the fractionation factor. The higher this ε value is, the more the δ ratio is affected. This reinforces that water column denitrification is one of the most highly fractionating processes in the water column, and that the $\delta^{15}N$ value is useful for seeing suboxic water conditions. Modified from Sigman and Casciotti, (2001).

In this study, for the measured $\delta^{15}N$ values, we are searching for more positive spikes before and after the event that would indicate suboxic water conditions and lower values during the OAE indicating anoxic or oxic water conditions. The use of $\delta^{15}N$ values with other stable isotope values to examine water column redox has been done before to successfully identify other OAEs in OM rich intervals (Rau et al., 1987; Jenkyns et al., 2001; Ohkouchi et al., 2006; Jenkyns et al., 2007; Juniam and Arthur, 2007).

Figure 9 shows a conceptual model of what the OAE 1d $\delta^{15}N$, $\delta^{13}C_{org}$, and TOC data might look like before, during, and after the event. The $\delta^{13}C_{org}$ will have lower values before OAE 1d begins. This is shown by the deepest interval on the figure and indicates less preservation and burial of organic matter (Scholle and Arthur, 1980; Leckie et al., 2002). As the water column becomes more depleted in dissolved oxygen, $\delta^{13}C_{org}$ values will increase and become the most positive during OAE 1d. This is because the increase in the $\delta^{13}C_{org}$ value can be interpreted as increased burial and preservation (Scholle and Arthur, 1980). The $\delta^{13}C_{org}$ value after OAE 1d will start to decrease as preservation and burial decreases. TOC values in this conceptual model follow the same overall trend of the $\delta^{13}C_{org}$ but are delayed by a small amount in Figure 9. This was done to show that although more TOC may be deposited, the trend might not follow the $\delta^{13}C_{org}$ curve exactly. Burial and preservation of organic matter, TOC in this case, during an OAE can vary depending on local depositional factors so that the TOC values will be elevated during the OAE, but not at the same time as the $\delta^{13}C$ value (Scott et al., 2013; Bottini and Erba 2018). The $\delta^{15}N_{acidified}$ value constrains redox conditions in this model. Before the event begins at the deepest interval of Figure 9, the $\delta^{15}N_{acidified}$ value will be more negative, because the water column should be oxic (Altabet and Francois, 1994; Quan et al., 2013b).

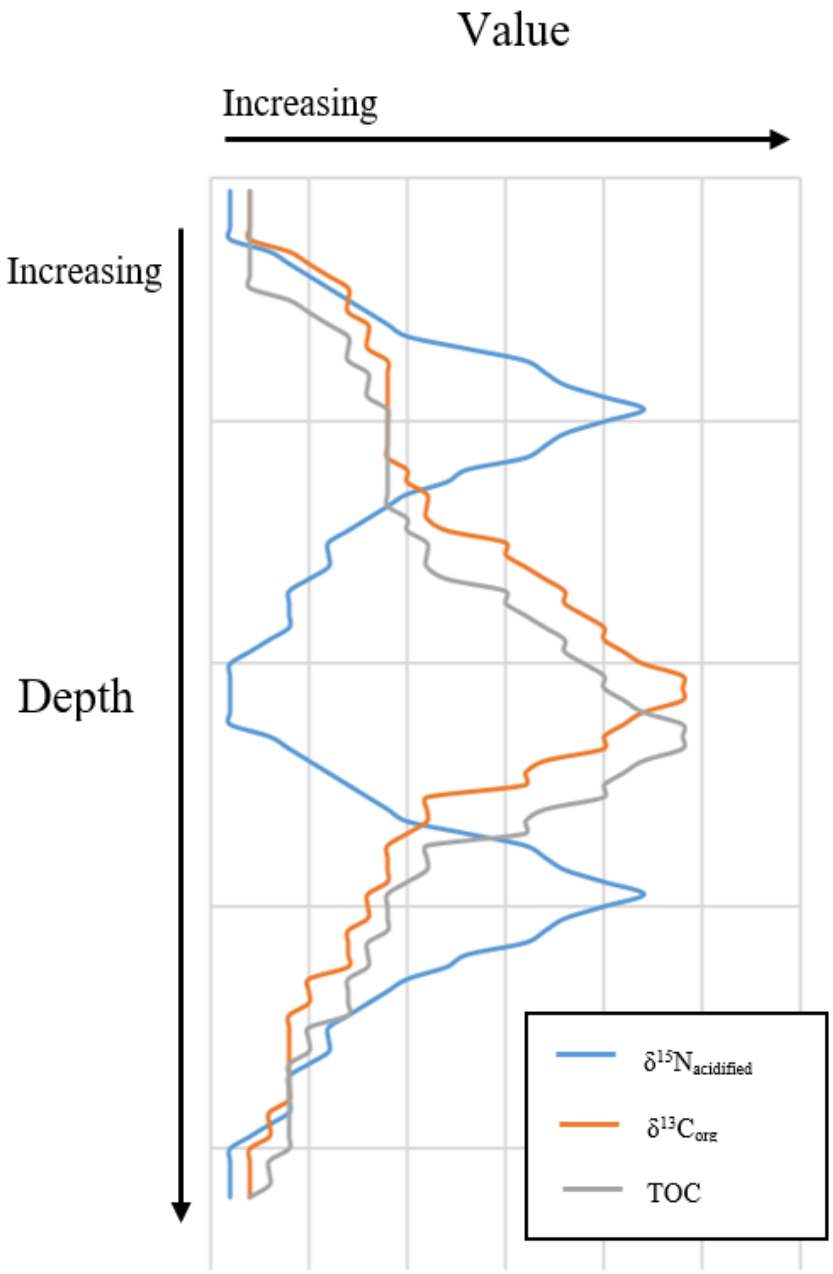

Figure 9. Conceptual model for an Ocean Anoxic Event 1d occurrence.

As the water column transitions from oxic to suboxic, a spike in $\delta^{15}N_{acidified}$ values will be seen before OAE 1d occurs. This is because denitrification is a highly fractionating process that displays more positive $\delta^{15}N$ values during suboxic conditions in bottom water redox in preserved sediments (Altabet and Francois, 1994; Quan et al., 2013b; Rivera et al., 2015). During OAE 1d, the $\delta^{15}N_{acidified}$ values will decrease due to anoxia, if the carbon values also increase and indicate an increase in burial and preservation (Rau et al., 1987; Jenkyns et al., 2001; Jenkyns et al., 2007; Juniam and Arthur, 2007; Juniam and Arthur, 2018).

After OAE 1d, the $\delta^{15}N_{acidified}$ values will increase again and a second suboxic spike will be seen, followed by a decrease in values. This indicates a transition from suboxic to oxic waters after OAE 1d (Altabet and Francois, 1994; Quan et al., 2013b; Rivera et al., 2015). While trends for $\delta^{15}N$ values might not always follow the conceptual model shown in Figure 9, this profile has been observed in at least one possible occurrence of an OAE (Junium et al., 2018). If similar trends are seen in the data which are shown in the conceptual model, then the trends should indicate that the redox conditions at the time of deposition were anoxic and that OAE 1d occurred at intervals within each Hole.

Geologic Setting

The most recent geologic reports and surveys of the Mentelle Basin were carried out by IODP Expedition 369 (Huber et al., 2019), publications from data collected from the expedition (Harry et al., 2020; Lee et al., 2020; Maritati et al., 2021) and Geoscience Australia (Borissova et al., 2010). The Mentelle Basin is a deep-water basin that formed in the early Permian and is a

component of an extensional rift system that developed during the breakup of Gondwana (occurring Paleozoic to Mesozoic) along Australia's current southwestern margin (Borissova et al., 2010; Harry et al., 2020; Maritati et al., 2021). The rift system was further shaped during the Triassic and early Jurassic by processes dominated by thermal subsidence (Borissova et al., 2010; Huber et al., 2019; Harry et al., 2020). Extension that occurred in the middle Jurassic led to the buildup of thick layers of sediments in half-graben depocenters (Borissova et al., 2010). The breakup of the supercontinent Pangea started in the Early Cretaceous (Borissova et al., 2010; Harry et al., 2020; Lee et al., 2020). Because of the Mentelle Basin's proximity to a triple junction, volcanic sediments from the continental breakup can be seen extensively in the western Mentelle Basin in the early Cretaceous, presumably transported through northward fluvial pathways that changed during the break up of India from Australia-Antarctica (Borissova et al., 2010; Harry et al., 2020; Maritati et al., 2021).

During the Hauterivian (132.9 - 129.4 Ma) through early Barremian, (129.4 Ma) the depositional environment of the Mentelle Basin started to change from a shelf to an upper bathyal setting (200 - 600 m), with decreasing terrestrial input (Lee et al., 2020). At approximately 126 Ma when the Indian and Australia-Antarctica plates separated, a further breakup of Gondwana occurred and seafloor spreading west of the Naturaliste Plateau began (Harry et al., 2020; Lee et al., 2020). During this time, the Naturaliste Plateau subsided quickly with a high sedimentation rate, so the depositional environment was still more shallow throughout the Hauterivian to early Barremian, corresponding to an upper bathyal setting (Lee et al., 2020). The deepening of the Mentelle Basin seems to correspond to a syn-rift subsidence associated with seafloor spreading in the northward Perth Abyssal Plain and its westward spread (Lee et al., 2020). After the final breakup of the

Australia-Antarctic plate from the Indian plate located to the west of the Naturaliste Plateau, the region maintained upper bathyal depths (600 - 2000 m) with low sedimentation rate during the late Barremian through early Aptian (125 Ma) (Harry et al., 2020; Lee et al., 2020).

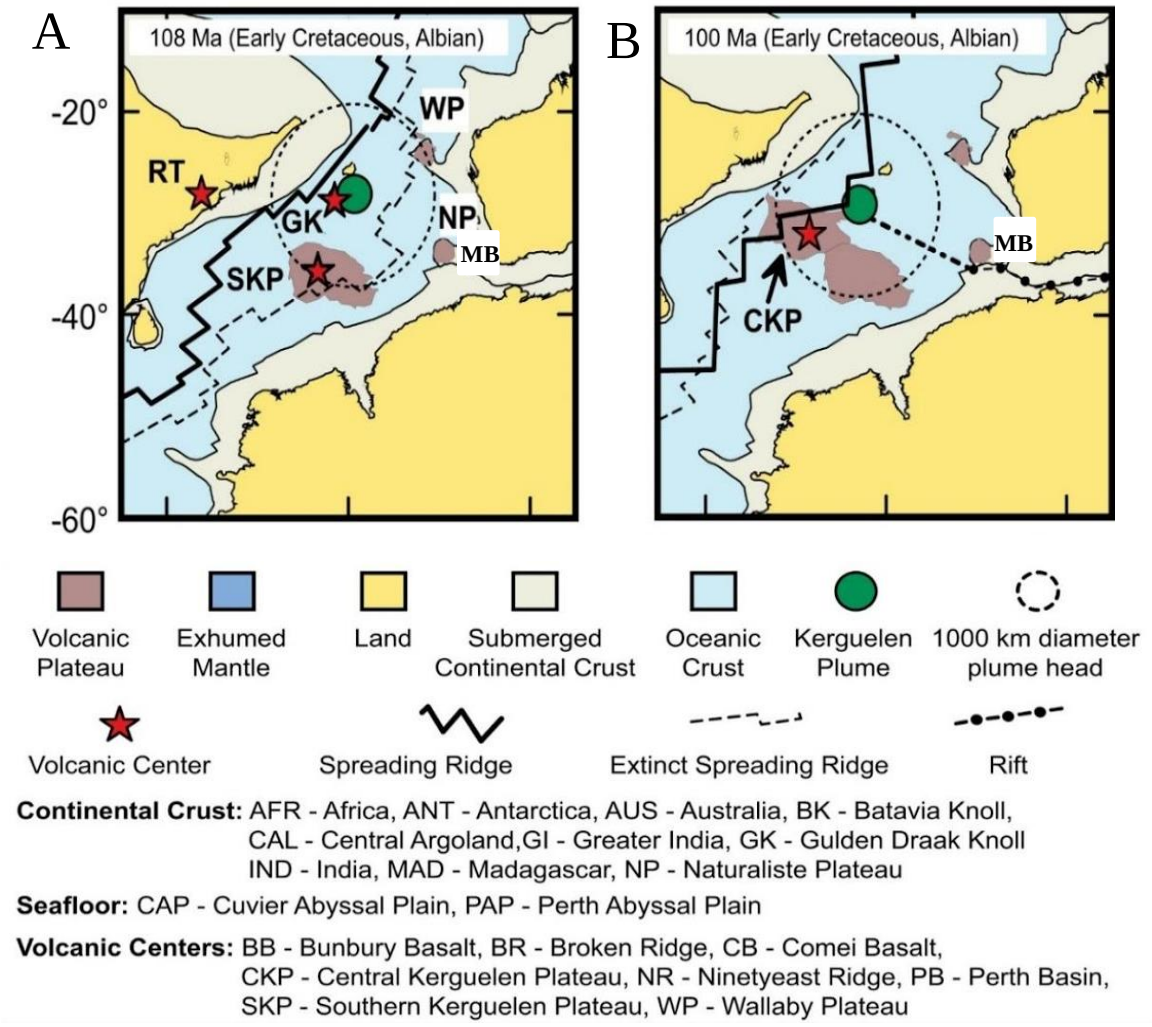

Figure 10. A reconstruction of the southwestern margin of Australia through the Albian and during OAE 1d (B) and after (A). The Mentelle Basin is denoted as MB on both A and B. The Mentelle Basin was in an area that had an exchange with the ocean because of the northward movement of the Indian plate opening the waterway, and there was a rift that was active during the time of OAE 1d (Modified from Harry et al., 2020).

During the Late Cretaceous or approximately 105 Ma, after the breakup, the margin of the Mentelle Basin subsided further. Seafloor spreading shifted from west of the Naturaliste Plateau to the southern Australian margin (Harry et al., 2020; Lee et al., 2020). During the time of OAE 1d (Albian-Cenomanian boundary), the Mentelle Basin was dominated by thermal subsidence while the Indian Ocean was spreading quickly (Borissova et al., 2010; Harry et al., 2020; Lee et al., 2020). Figure 10 shows the area around the Mentelle Basin (MB) a few million years before (Figure 10A) and during OAE 1d (Figure 10B). The Mentelle basin at the time of OAE 1d was defined as middle to lower bathyal depths (600 – 2000 m) (Lee et al., 2020). The lithologies for both Holes U1513C and U1516C can be seen in Figures 11 and 12 respectively and are both classified as claystones that are nannofossil rich (Huber et al., 2019). Claystone layers are usually deposited in low energy environments that are consistent with a deeper basin (Dill, 2020). The deposition of claystones in the Albian (113 – 100 Ma) and during OAE 1d suggests that post rift thermal subsidence which started in the late Aptian (113 Ma) affected sedimentation and that the spreading center moved westward from the southwest to the southern Australian margin (Lee et al., 2020).

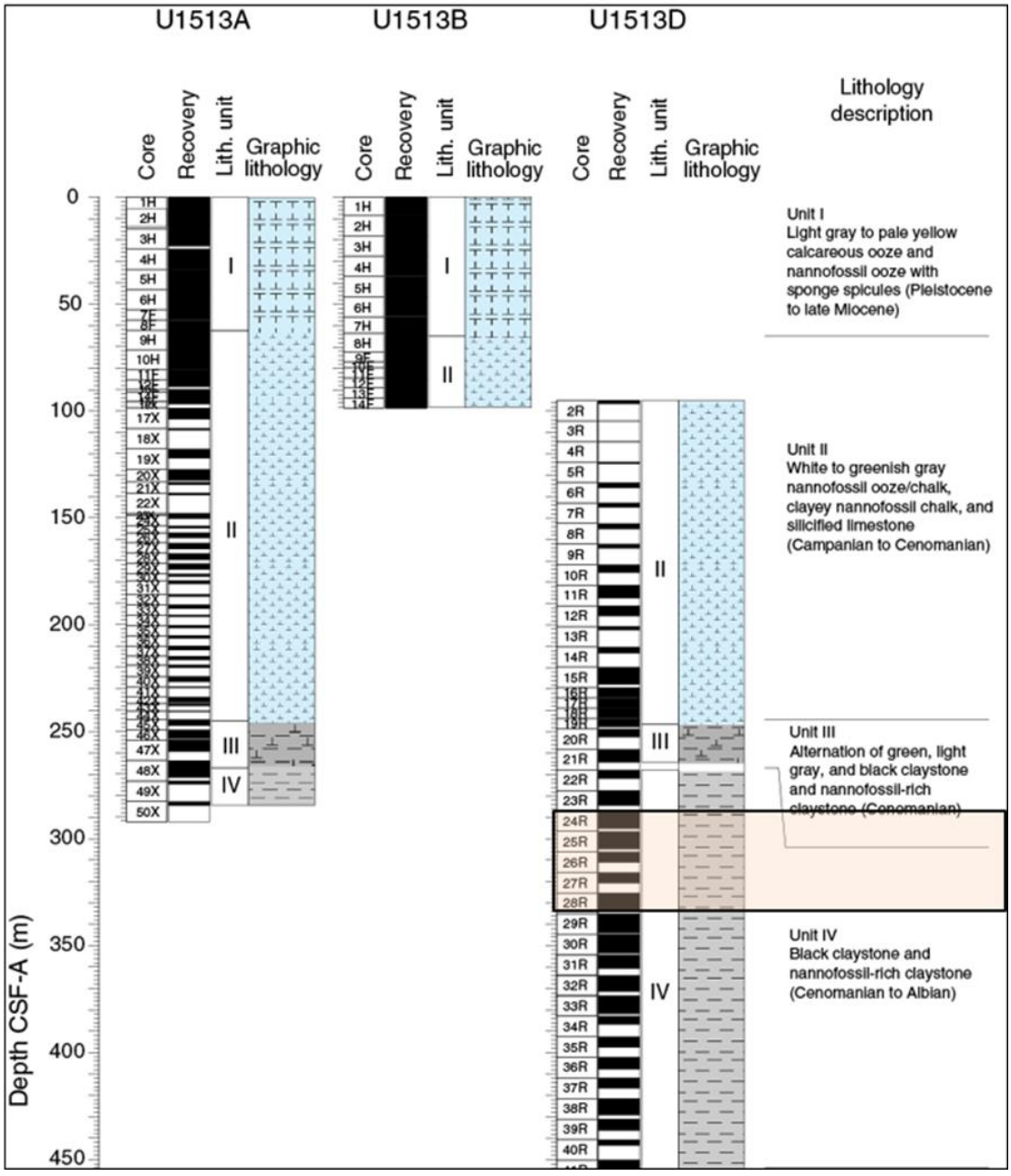

Figure 11. Stratigraphic column for Site U1513. Hole U1513D is used in place of Hole U1513C. The cores from Hole U1513C are dedicated for future measurements; they were immediately preserved upon recovery and not described onboard. The orange boxed off area is the interval for the hole used in this research (Huber et al., 2019).

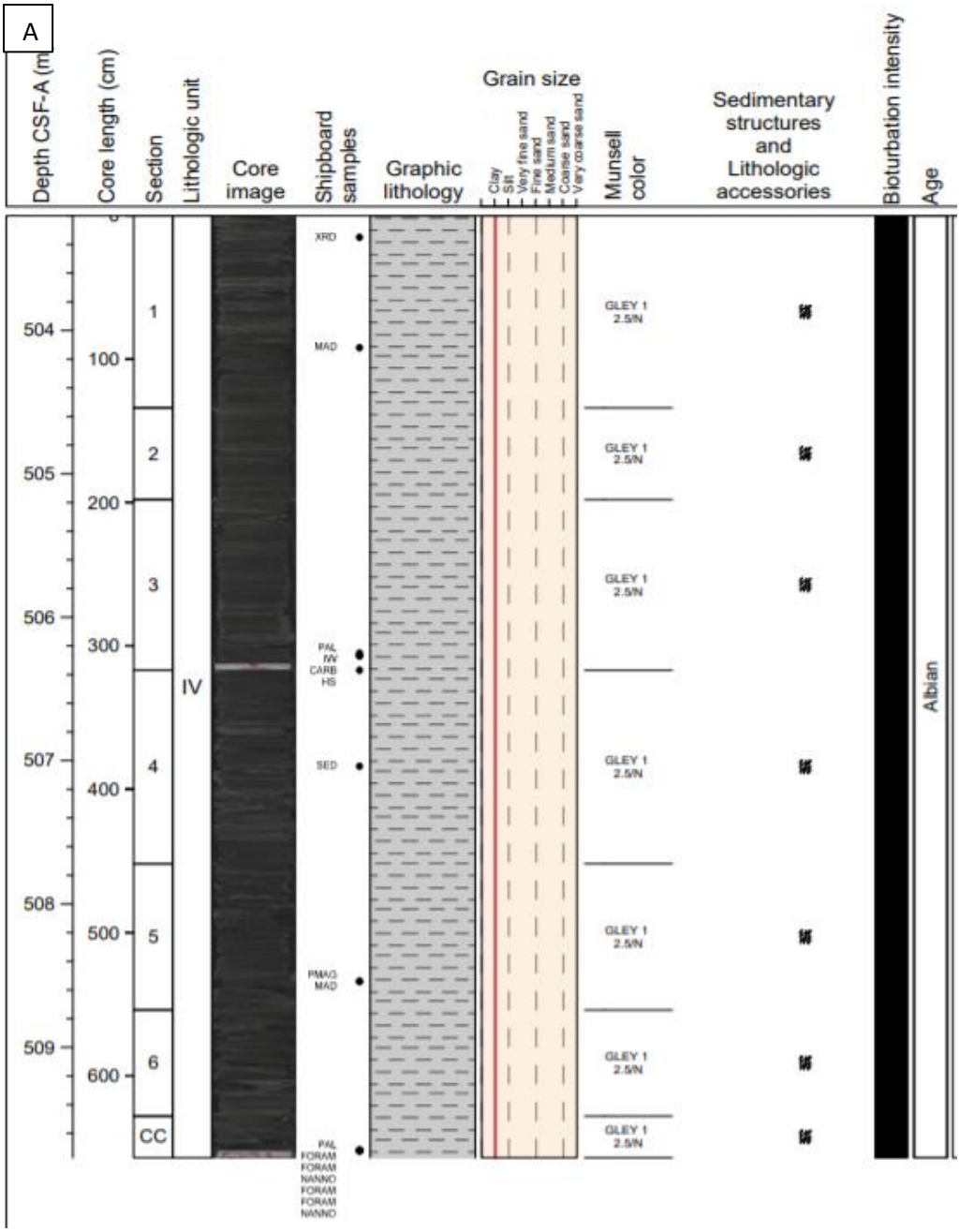
A
Depth CSF-A (m)
Core length (cm)
Section
Lithologic unit
Core image
Shipboard samples
Graphic lithology
Grain size
Clay
Silt
Very fine sand
Fine sand
Medium sand
Coarse sand
Very coarse sand
Munsell color
Sedimentary structures and Lithologic accessories
Bioturbation intensity
Age
504
505
506
507
508
509
100
200
300
400
500
600
1
2
3
4
5
6
CC
IV
XRD
MAD
PAL
NN
CARB
HS
SED
PMAG
MAD
PAL
FORAM
FORAM
NANNO
FORAM
FORAM
NANNO
GLEY 1 2.5/N
Albian

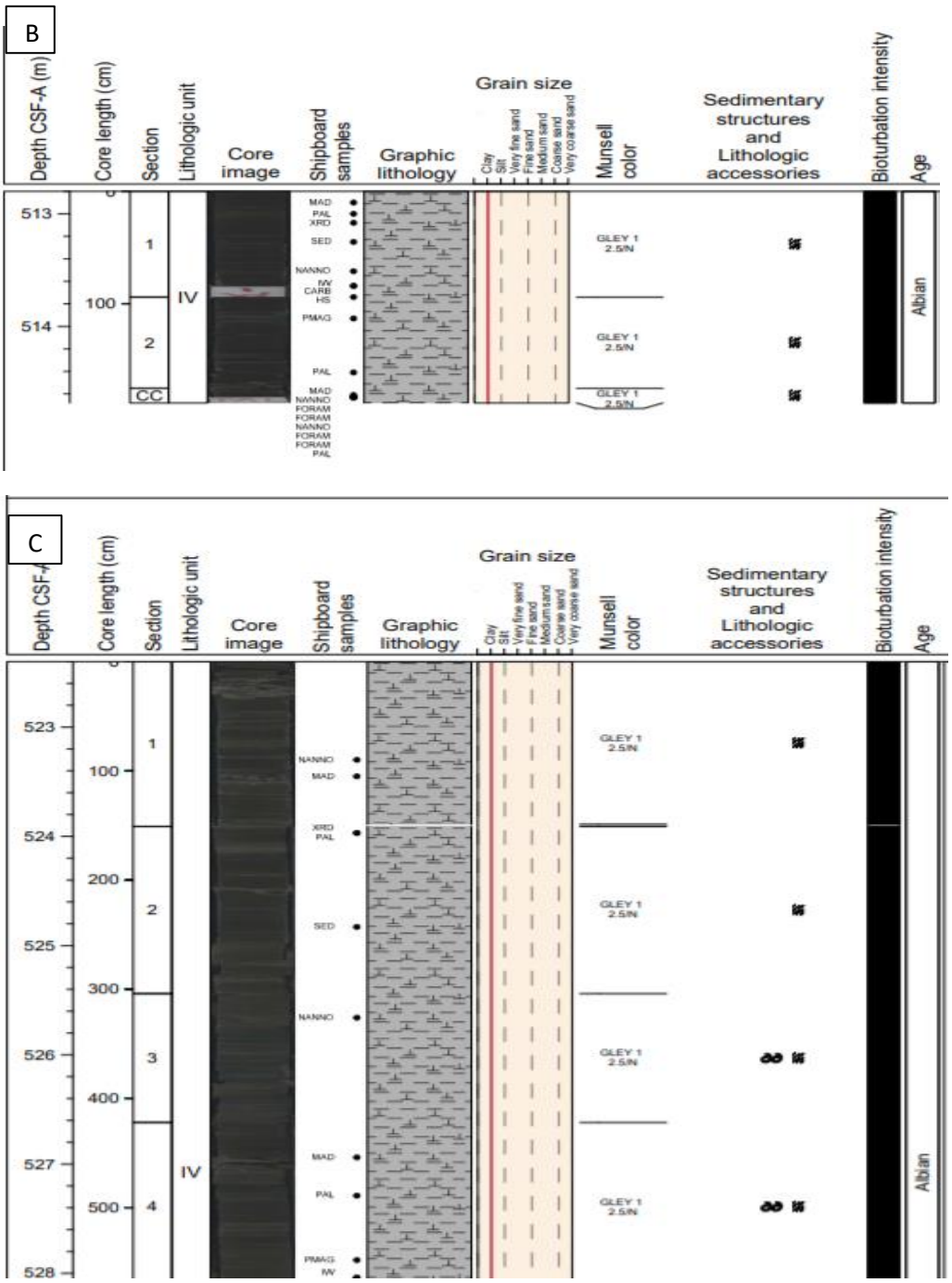

Figure 12. Stratigraphic column Hole U1516C A 38R, B 39R, C 40R. All are classified as lithological unit IV (Huber et al., 2019).

CHAPTER III

METHODOLOGY

Samples taken from IODP Expedition 369 from two different locations, Hole U1513C and Holes U1516C, are used in this study. The depth range for the samples from Hole U1513C is 294.89 to 333.70 meters. Figure 13 shows the approximate age of the sediments from Hole U1513C (Huber et al., 2019). The sediments from Hole U1516C used in this study range in depth from 503.67 to 527.75 meters. Age approximation of the samples is shown in Figure 14 in relation to depth (Huber et al., 2019). The sample intervals from both Holes U1513C and U1516C are both approximately 100 to 102 Ma, which is a similar time as OAE 1d's occurrence (Petrizzo et al., 2008; Jenkyns, 2010; Scott et al., 2013). The samples that were used to attempt to capture the OAE 1d interval were split between two sites with 140 from Hole U1513C, with a depth range of 294.89 – 334.7 meters and 80 from Hole U1516C with a depth range of 503.64 – 527.75 meters. The samples were run in loads that consisted of 25 samples with two duplicates per sample run along with the appropriate number of standards. After many trials, two data points for $\delta^{15}N_{acidified}$, 1513-27R-2w – 27/29 and 1513-27R-2w – 116/118 were not able to be measured.

Analysis of these samples is a team effort; Dr. Tracy M. Quan's team is tasked with measuring stable isotopes such as $\delta^{15}N$, Dr. Laurent Riquier's team is testing the samples for trace metals and Dr. Zhaokai Xu's team is analyzing the sediment grain size distribution and composition. The samples were divided among the three groups of scientists, to give each at least 5 grams to run

their respective tests. Over these selected intervals, there are 220 samples from two different Holes, U1513C and U1516C.

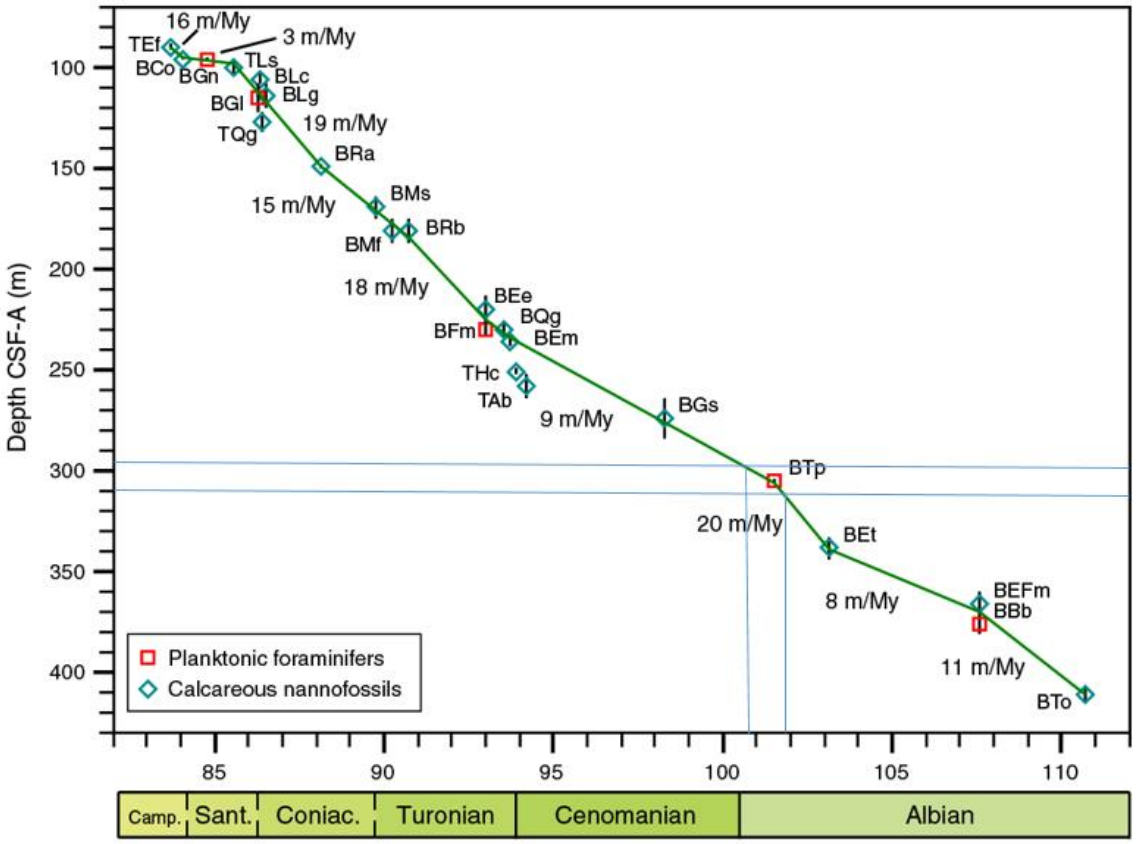

Figure 13. Approximate age of Hole U1513C using planktonic foraminifera to date. Cores from Hole U1513D were used to correlate approximate ages of the samples for Hole U1513C. The correlation could be done because cores from depths of 292.91 to 320.19 meter from Hole U1513D, indicated by the blue lines, could be used for U1513C because their recovery at the same interval for this research is over is 100% (Huber et al., 2019).

The dry sediments were crushed and homogenized using an agate mortar and pestle. The dry sediments were put into an oven to dry for approximately 24 hours at 60° C. After this initial drying, the samples were put through the acidification process. The samples, ranging from 50-55 grams, were packaged into silver (Ag) capsules and treated with a drop of distilled water (DI)

water and a drop of 37% hydrochloric acid (HCl) for both $\delta^{15}N_{acidified}$ and $\delta^{13}C_{org}$ analyses. The samples were then put into an oven until completely dry, usually for 24 hours.

The acidification was done until no significant effervescence was seen in the samples, usually requiring two rounds (Brodie et al., 2011). Once the acidification process was completed, vanadium pentoxide (V_2O_5) was added to the capsule to act as a catalyst. Then the silver capsules and all standards were wrapped and covered by tin capsules.

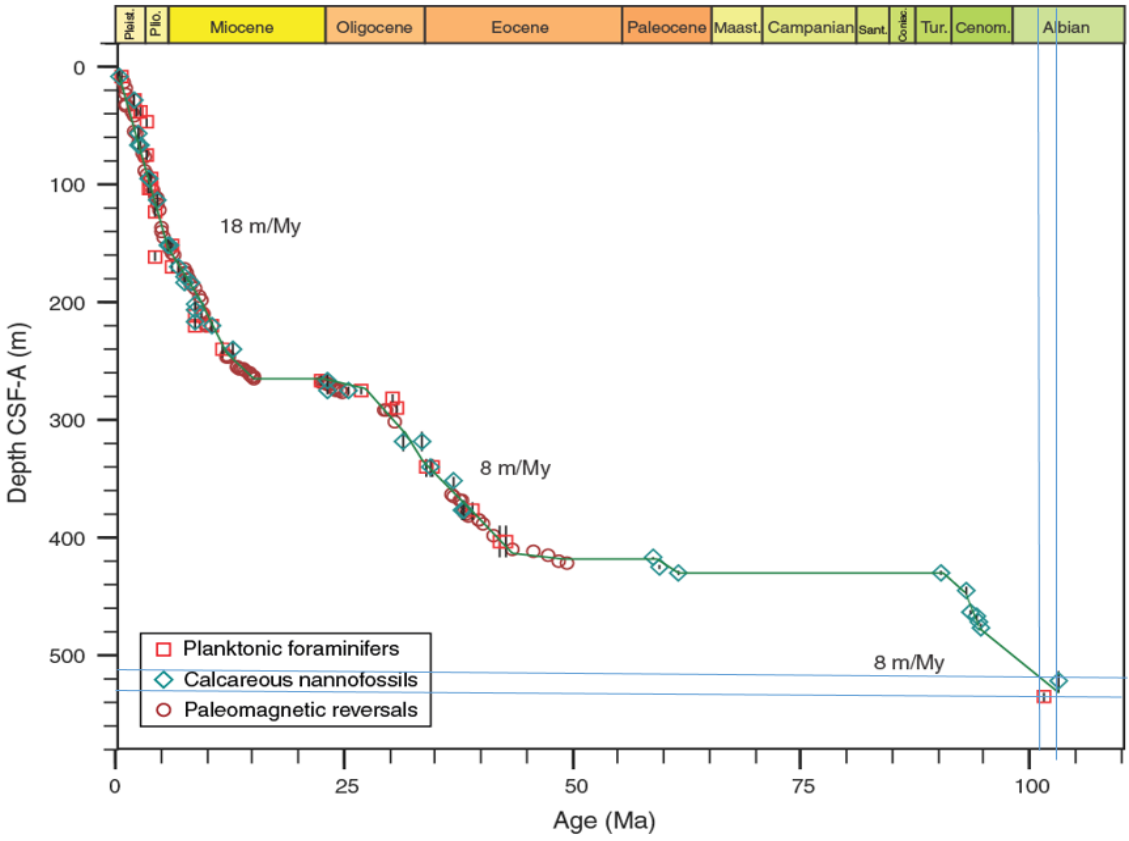

Figure 14. Approximate age of Hole U1516C using planktonic foraminifera to date. The core's range is 503.64 to 527.75 meters, which are indicated by the blue lines (Huber et al., 2019).

The $\delta^{15}N_{acidified}$ and $\delta^{13}C_{org}$ were measured during separate runs using a Costech Elemental Analyzer connected to a ThermoFinnegan Deltaplus XL Isotope Ratio Mass Spectrometer (EA-

IRMS). The use of the subscript acidified for the $\delta^{15}N$ value, $\delta^{15}N_{acidified}$, is to differentiate it from other nitrogen value methods, such as $\delta^{15}N_{bulk}$, and describe the method used to gather the values (Brodie et al., 2011). For this study, an emphasis must be made that we use $\delta^{15}N_{acidified}$ (Brodie et al., 2011). This means that we cannot directly compare $\delta^{15}N_{bulk}$ sediment numerical values to the $\delta^{15}N_{acidified}$ numerical values collected during this research, but we can compare overall trends with other studies that use other $\delta^{15}N_{bulk}$ values. The reason $\delta^{15}N_{acidified}$ cannot be directly compared to $\delta^{15}N_{bulk}$ is that during the process of acidification, some organic matter containing nitrogen could be destroyed. This is why the subscript $\delta^{15}N_{org}$ meaning $\delta^{15}N$ organic for the data collected in this study cannot be used, as there is not enough confidence that some organic matter containing nitrogen is not destroyed in the process (Brodie et al., 2011). The $\delta^{15}N_{acidified}$ method is only used when samples are low in organic matter, which means acquisition of $\delta^{15}N_{bulk}$ was not possible during the course of this research project (Brodie et al., 2011).

Instrument error is ± 0.4 ‰ or less and is estimated from the standard deviation of a set of repeat measurements of the standards. The sediment error is ± 0.7 ‰ or less and is estimated from the standard deviations of duplicate samples that were included in each use of the EA-IRMS for sample acquisition. The standard deviations for each error are displayed in the Appendix in Tables C for instrument error and D for sediment error.

The L-glutamic acid USGS-40 RM8753 or USGS-40 as shorthand was used as a standard in sample runs for both nitrogen and carbon isotope standards. The IAEA-N3 KNO_3 RM8574 or IAEA-N3 for short is a standard used for nitrogen runs and the UREA #1 was used in the carbon run. Acetanilide was used as a concentration standard and is composed of both nitrogen and

carbon. The definition for the general calculation for δ ratios for stable isotopes is displayed in Figure 15A. The specific definition of the calculation for $\delta^{15}N$ generally is shown in Figure 15B.

A.

$$\delta\ (‰) = \frac{R_{sample}}{R_{standard}} - 1$$

B.

$$\delta^{15}N\ (‰) = \frac{{}^{15}N\ /\ {}^{14}N_{sample} - {}^{15}N/{}^{14}N_{atm.\,N_2}}{{}^{15}N\ /\ {}^{14}N_{atm.\,N_2}} \times 1000$$

Figure 15. A. How a δ ratio is calculated generally for isotope R. Modified from Sigman and Casciotti, (2001). B. How $\delta^{15}N$ ratio is calculated. Modified from Altabet and Francois, (1994).

CHAPTER IV

RESULTS

Figures 16 and 17 show the $\delta^{15}N_{acidified}$ profiles for the entirety of Hole U1513C (Figure 16) and the suspected OAE 1d interval for Hole U1513C (Figure 17). Figures 18 and 19 show the $\delta^{15}N_{acidified}$ profiles for the entirety of Hole U1516C (Figure 18) and the suspected OAE 1d interval for Hole U1516C (Figure 19). In these figures, the data points are connected by lines if the gap is not larger than a meter. This is done so that an overall trend can be seen and not because the data points are necessary continuous. This could be because of problems with coring, which created gaps or hiatuses for certain areas that were not recovered. A concern with intervals of core missing is that if the hiatus is large enough, a possible OAE might not have been captured.

The overall representation of the redox state at Hole U1513C is variable. The $\delta^{15}N_{acidified}$ profile is shown in Figure 16, and ranges from -1.2 ‰ to 2.2 ‰. The average $\delta^{15}N_{acidified}$ value is 0.1 ‰. Throughout this Hole, the $\delta^{15}N_{acidified}$ values fluctuate with no clear trends of $\delta^{15}N_{acidified}$. Figure 17 shows the suspected OAE 1d interval and contains both the minimum and maximum values for this Hole. The samples in Figure 17 were sampled at a higher resolution than other parts of the data set at this Hole. The suspected OAE interval for Hole U1513C contains both the minimum and maximum for the entire data range and has an average $\delta^{15}N_{acidified}$ value of -0.05 ‰. The change in $\delta^{15}N_{acidified}$ values for U1516C is generally less than 1 ‰ and only ranges from -1.2 ‰ to 0.7 ‰ (Figure 18). The average $\delta^{15}N_{acidified}$ value is -0.3 ‰. The suspected OAE interval for

Hole U1516C contains both the minimum and maximum for the entire data range and has an average $\delta^{15}N_{acidified}$ value of -0.4 ‰.

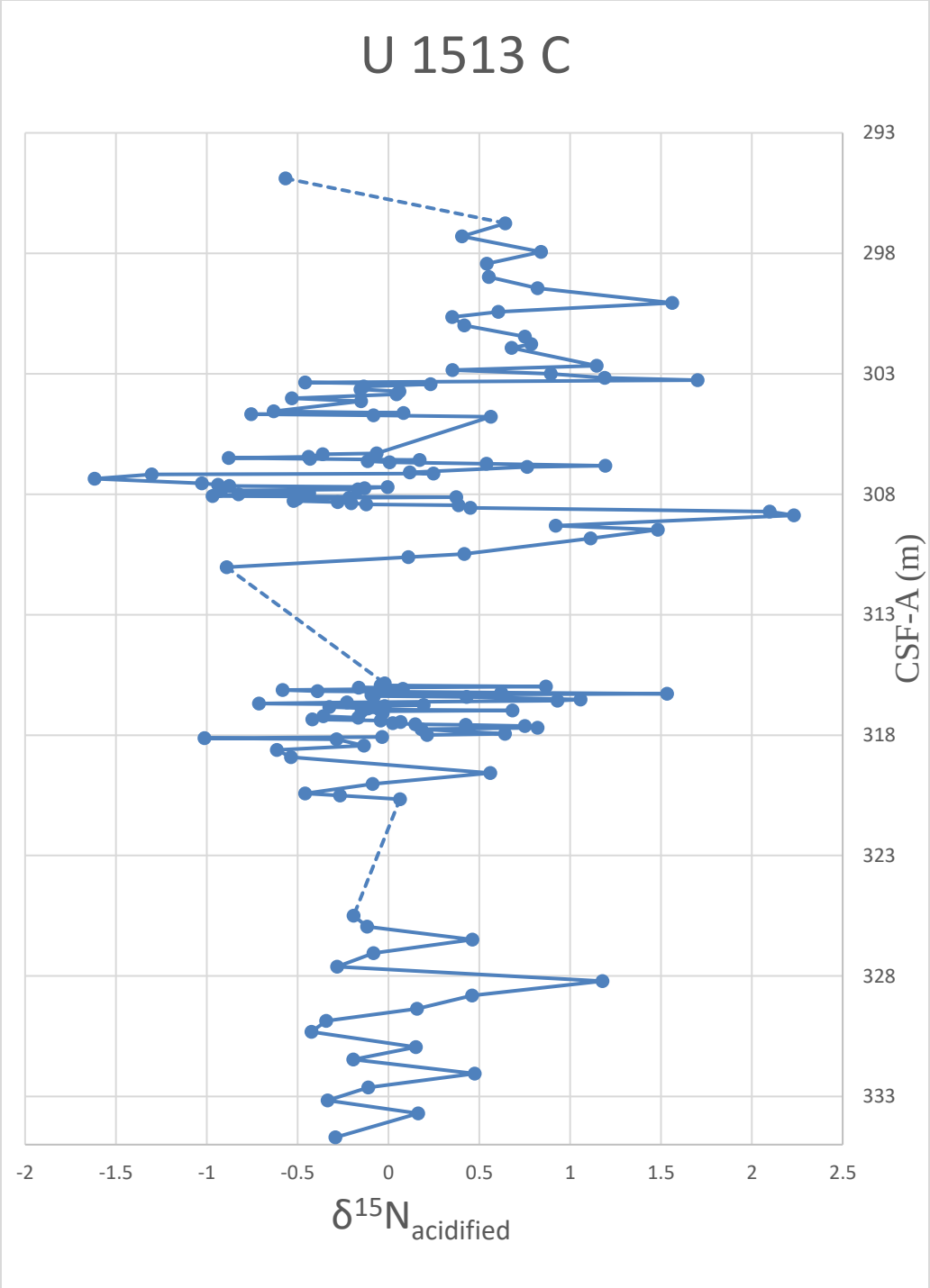

Figure 16. $\delta^{15}N_{acidified}$ profile for U1513C. Hiatus is represented by a dotted line when there is more than a meter gap between sample points. The depth range is 294.89 – 334.7 m.

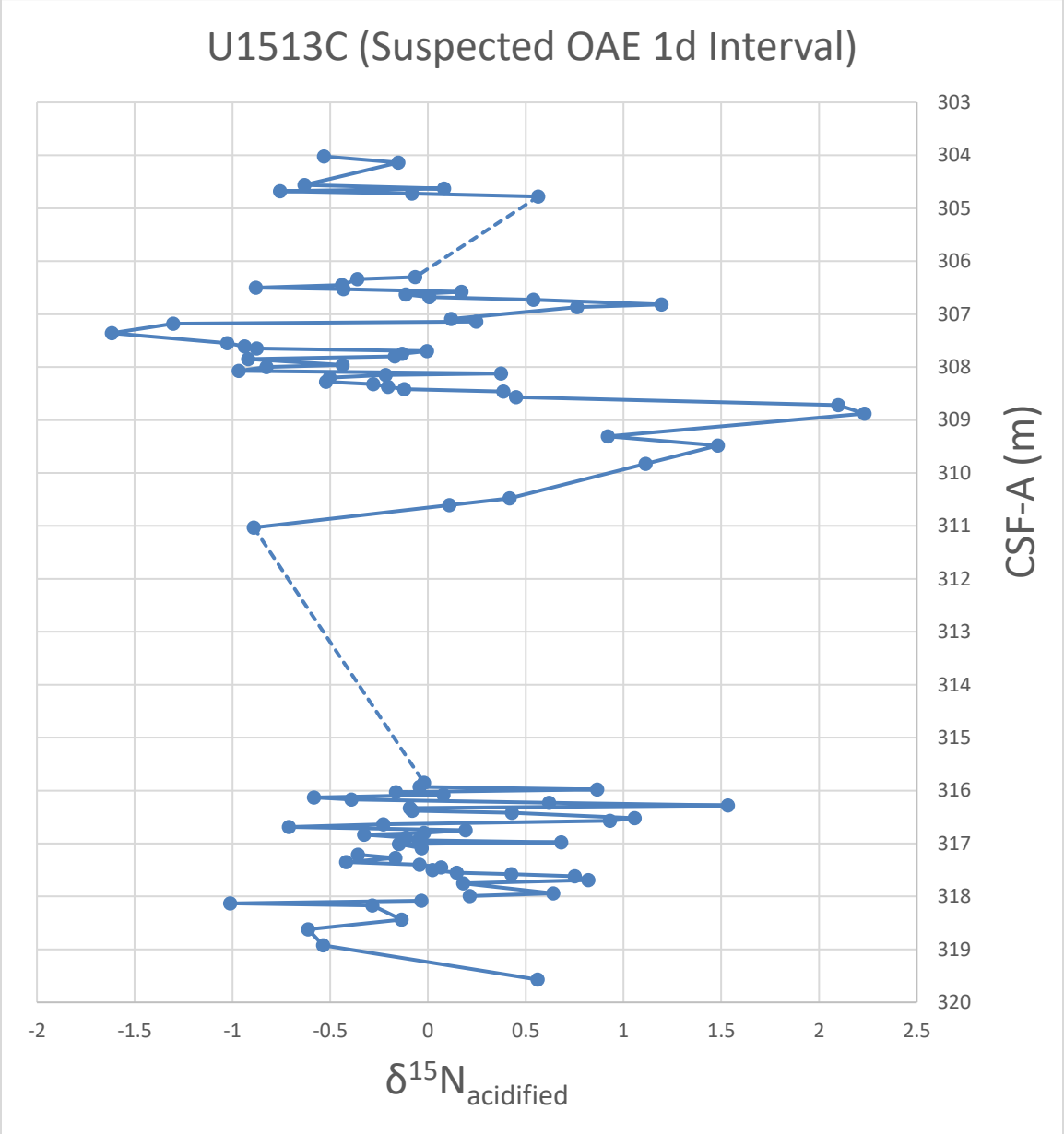

Figure 17. $\delta^{15}N_{acidified}$ profile for possible OAE 1d interval for U1513C. Hiatus is represented by a dotted line when there is more than a meter gap between sample points.

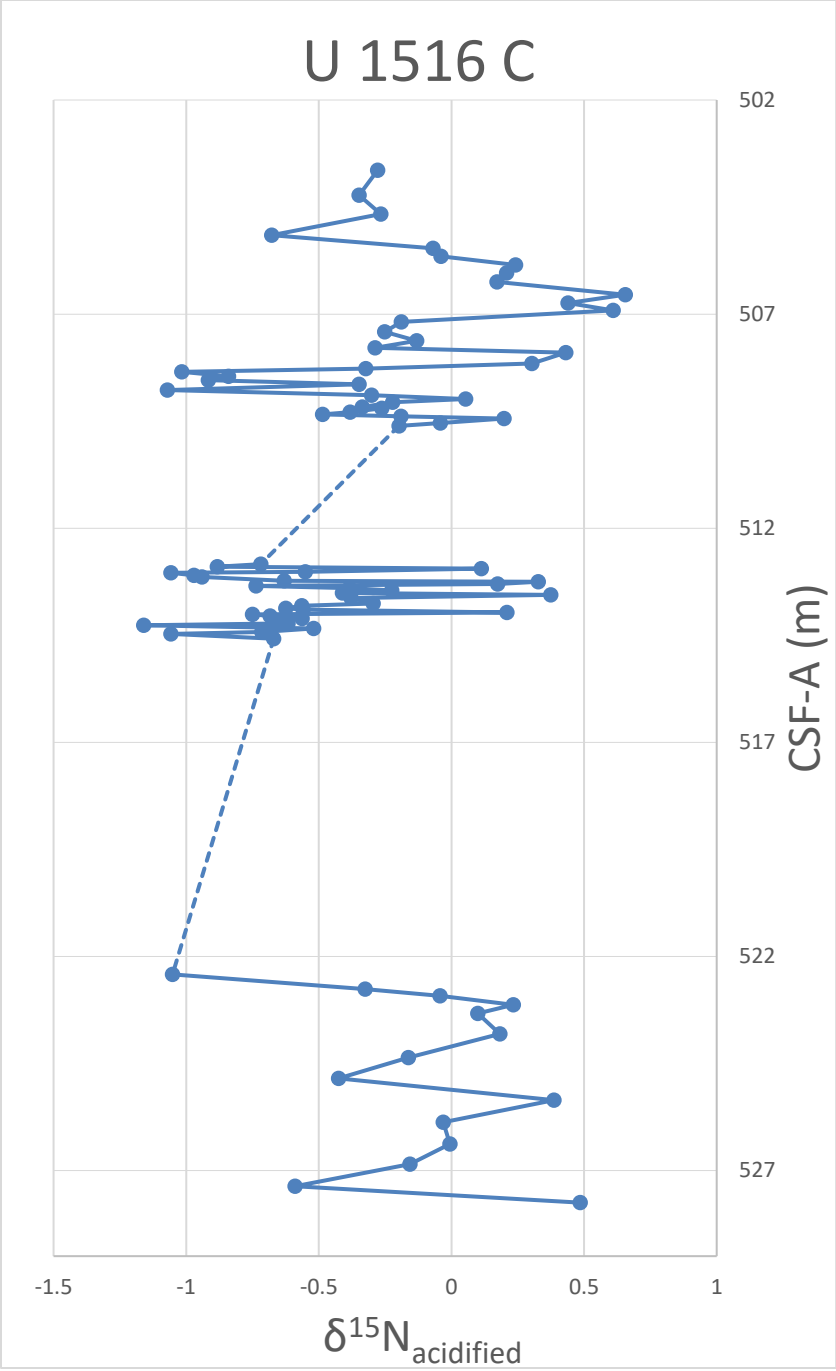

Figure 18. $\delta^{15}N_{acidified}$ profile for U1516C. Hiatus is represented by a dotted line when there is more than a meter gap between sample points. The depth range is 503.64 – 527.75 meters.

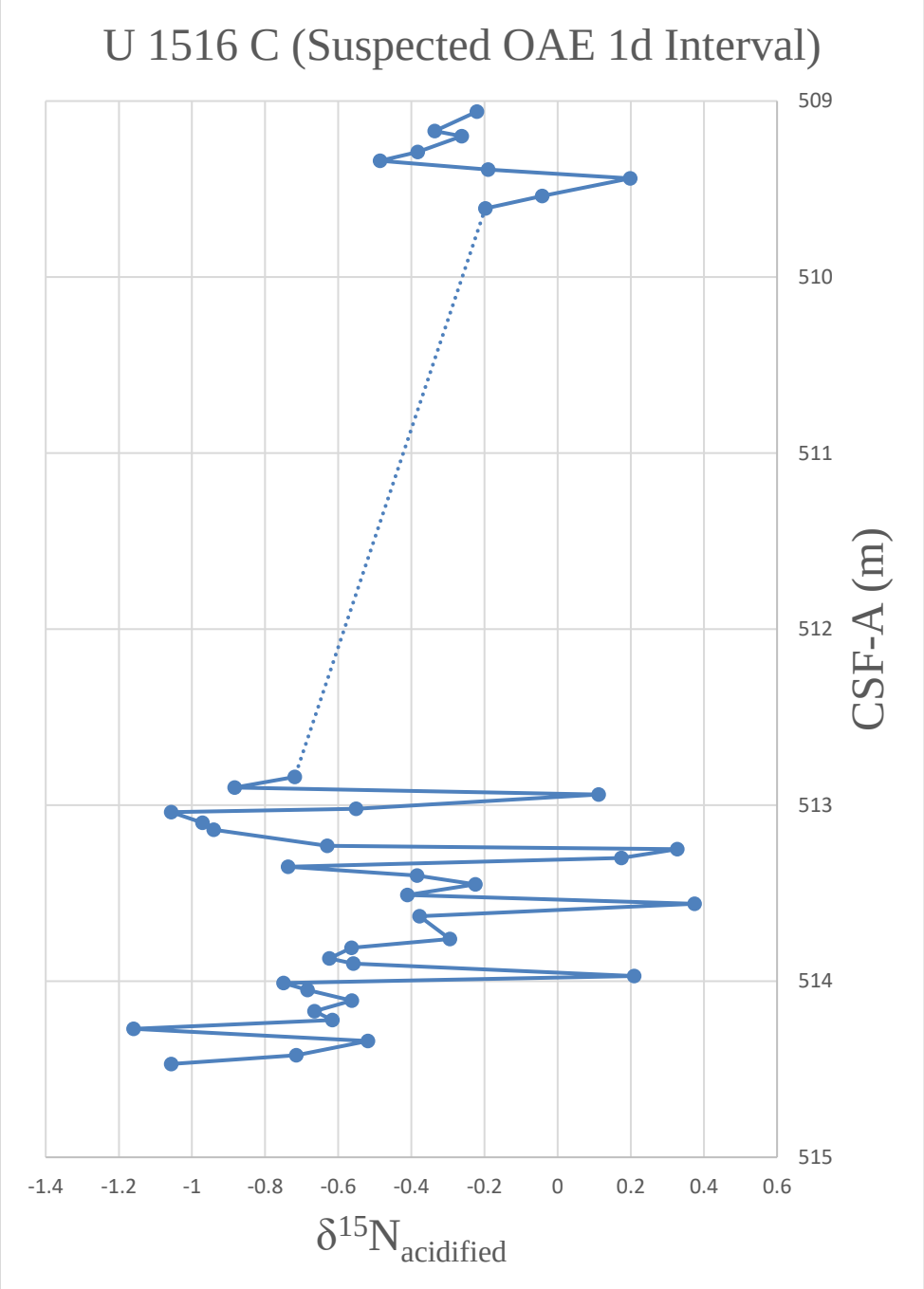

Figure 19. $\delta^{15}N_{acidified}$ profile for possible OAE 1d interval for U1516C. Hiatus is represented by a dotted line when there is more than a meter gap between sample points.

CHAPTER V

DISCUSSION

The primary focus of this research project was to investigate the occurrence of Ocean Anoxic Event 1d in the Mentelle Basin using $\delta^{13}C$, TOC, and $\delta^{15}N$. The proxy that was measured in this study was $\delta^{15}N_{acidified}$.

U1513C

In Figure 17, there is one section that might show a possible trend for $\delta^{15}N_{acidified}$ values, as discussed in the conceptual model, Figure 9. The trend seen is two more positive values of $\delta^{15}N_{acidified}$, which peak at values 1.2 ‰ at depth 306.82 meters and 2.2 ‰ at depth 308.88 meters, with an average of 1.7 ‰ and standard deviation of 0.5. The $\delta^{15}N_{acidified}$ values in between the peaks have a minimum of -1.6 ‰ and a maximum of 0.4 ‰, with an average of -0.3 ‰ and a standard deviation of 0.8. The possible suboxic spikes flank more negative values, which have a minimum of -1.6 ‰ and a maximum of 0.4 ‰. The values in the more negative interval vary more than 1 ‰ from the two more positive peak values. The more negative values in between the more positive spikes of $\delta^{15}N_{acidified}$ could be oxic or anoxic, following the trend seen in Figure 3 (Altabet and Francois, 1994; Sigman and Casciotti, 2001; Quan et al., 2013a; Quan et al., 2013b; Rivera et al., 2015). Without at least one other proxy, specifically $\delta^{13}C$, we cannot determine if OAE 1d occurred at this interval (Rau et al., 1987; Jenkyns et al., 2001; Ohkouchi et al., 2006; Jenkyns et al., 2007; Juniam and Arthur, 2007). There is a hiatus in Hole U1513C in the

suspected OAE 1d interval, from depths of 311.03 - 315.85 meters (Figure 11), because of drilling error (Huber et al., 2019). Because this hiatus is in the suspected OAE 1d interval, there is a chance that an occurrence of OAE 1d was in the lost interval.

Hole U1516C

The overall trend seen at Hole U1516C is that the redox state is not that variable. Throughout this Hole, the $\delta^{15}N_{acidified}$ values do fluctuate, but not much; there is no clear trend seen that resembles the conceptual model, Figure 9. Figure 19 shows the suspected OAE 1d interval and contains both the minimum and maximum values for this Hole. There are some spikes in the values, but the largest changes are ± 1 ‰ and the values are all close to 0 ‰, which are values that can be associated with oxic or anoxic conditions (Altabet and Francois, 1994; Sigman and Casciotti, 2001). This is because a 0 ‰ value for $\delta^{15}N$ indicates that N_2 fixation could be occurring in an anoxic environment or that nitrification is occurring in an oxic environment (Altabet and Francois, 1994; Karl and Michaels, 2001; Sigman and Casciotti, 2001). Because the samples are lacking in organic matter, the more reasonable interpretation is that Hole U1516C was oxic throughout the interval for OAE 1d and throughout the entirety of the Hole. In the suspected OAE 1d interval for this Hole, there is a large hiatus from 509.61 - 512.84 meters (Figure 19). The missing interval is a significant portion of the suspected OAE 1d interval, approximately 60%, and there is a possibility there was a change in redox state, but the interval was not captured due to drilling error (Huber et al., 2019).

Preliminary data for $\delta^{13}C_{org}$ obtained through personal communication with Dr. Macleod and Dr. Hasegawa included an interval suspected to contain OAE 1d at Hole U1516C, ranging from approximately 506 - 523 meters (Dr. Macleod and Dr. Hasegawa, personal communication, April, 2019). The preliminary data show fluctuations between -25 ‰ to -27 ‰ for $\delta^{13}C_{org}$, reasonable values for organic rich intervals that have been shown to contain OAE 1d occurrences at other sites (Rau et al., 1987; Giraud et al., 2003; Petrizzo et al., 2008; Walther, 2009; Jenkyns, 2010; Scott et al., 2013). Another interpretation of the preliminary $\delta^{13}C_{org}$ values indicates the organic matter is marine in origin (Scholle and Arthur, 1980; Jenkyns, 2010). An occurrence of OAE 1d is not seen in this interval and more than one proxy is needed for a more robust and definitive discussion of redox state and possible OAE 1d occurrences.

General Discussion

The $\delta^{15}N_{acidified}$ data for Hole U1516C does not vary as much as compared to Hole U1513C. The range pf $\delta^{15}N_{acidified}$ values for Hole U1513C is 3 ‰, whereas for Hole U1516C $\delta^{15}N_{acidified}$ values are generally near 0 ‰ and fluctuate ± 1 ‰, with a range of 1.9 ‰. Hole U1516C might have had a more stable and less dynamic environment, which could be caused by several mechanisms, such as regional rifting and the Hole's position on the slope at the time of OAE 1d (Harry et al., 2020; Lee et al., 2020). Before OAE 1d, the basin was neritic, the photic zone that extends from the coast to the continental shelf, to the upper bathyal (Harry et al., 2020; Lee et al., 2020). After and during OAE 1d, the Mentelle Basin subsided and the water depth increased to at least middle bathyal depth (Harry et al., 2020; Lee et al., 2020). In addition, both Sites U1513 and U1516 went through a period of relatively quick sedimentation from 110 - 100 Ma (Harry et al., 2020). The

increase of sedimentation is proposed to be influenced by the onset of rifting on the southern margin between Australia and Antarctica around 100 Ma (Harry et al., 2020; Lee et al., 2020). The opening of the Australian-Antarctic gateway was occurring throughout the Mid-Cretaceous, including during OAE 1d, as seen in Figure 10B. The Mentelle Basin and surrounding areas have been shown to have restricted water circulation, as the Indian plate was moving north during the Albian (Harry et al., 2020; Lee et al., 2020) and as seen in Figure 10. Factors such as more restricted water circulation, the depths of the Holes during OAE 1d (600 – 2000 m), and a low depositional energy environment, indicate that the Mentelle Basin was an area that was favorable for anoxic conditions and a possible OAE occurrence (Wilson and Norris, 2001; Jenkyns, 2010; Scott at al., 2013; Bottini and Erba, 2018; Harry et al., 2020; Lee et al., 2020a). However, in this study the sediments from the Holes have low organic matter. Organic matter is better preserved in low oxygen conditions (Scholle and Arthur, 1980; Wilson and Norris, 2001; Leckie et al., 2002; Scott at al., 2013; Bottini and Erba, 2018), and the lack of organic matter could indicate that the Holes were oxic throughout the selected intervals or that alteration by other sources such as rifting or diagenesis could have altered the $\delta^{15}N_{acidified}$ signal after lithification (Rau et al., 1986; Altabet and Francois, 1994). The lack of organic matter was discovered through the method which was used to obtain the $\delta^{15}N_{acidified}$ values for both Holes (Bordie et al., 2011). This limited the interpretation of the $\delta^{15}N_{acidified}$ values because only general trends in the $\delta^{15}N_{acidified}$ data could be compared to $\delta^{15}N_{bulk}$ values. The Mentelle Basin, an area that appeared to have features that might foster an OAE 1d occurrence, does not seem to have recorded OAE 1d in Hole U1516C, and only a possible OAE 1d occurrence in Hole U1513C, shown through interpretation of $\delta^{15}N_{acidified}$ values. The possible occurrence of OAE 1d at Hole U1513 is based on one proxy, $\delta^{15}N_{acidified}$, in this research project. The main identifier of OAE 1d is a positive excursion of $\delta^{13}C$

and TOC during the event (Scholle and Arthur, 1980; Jenkyns, 2010; Petrizzo et al., 2008; Scott et al., 2013) and until those proxies measured, OAE 1d cannot be said to definitively occurred at the Mentelle Basin.

Conclusion

In this study, we speculate from $\delta^{15}N_{acidified}$ values that there is a possible occurrence of OAE 1d at Hole U1513C and Hole U1516C was possibly oxic. Hole U1513C could have had OAE 1d occur because there was an interval of $\delta^{15}N_{acidified}$ values resembling the trend seen in the conceptual model, Figure 9. With more publications from IODP Expedition 369, more information about the paleo position and paleoenvironment of the Mentelle Basin will be learned, but after this research and the publication of Harry et al., (2020), Lee et al., (2020), and Maritati et al., (2021), the paleoenvironment of both Holes can only be constrained to a basin with depths of approximately 600 - 2000 meters with a low energy regime at the time of deposition (Huber et al., 2019; Dill et al., 2020). The effect that nearby rifting had on the Mentelle Basin has been shown to have caused subsidence and deepening of the basin throughout the Cretaceous (Borissova et al., 2010; Huber et al., 2019; Harry et al., 2020; Lee et al., 2020). Investigation of other factors that can influence or constrain redox conditions would be very important to be examined in future studies. The most important proxies yet to be measured for this sampling interval are $\delta^{13}C_{org}$ and TOC. Without these proxies, OAE 1d cannot be said to have occurred at the Mentelle Basin. There have been studies in which the analysis of OAEs have been limited to $\delta^{15}N$, $\delta^{13}C$, and other measurements of nitrogen and carbon, such as C/N weight ratios or TOC (Rau et al., 1987; Jenkyns et al., 2001; Jenkyns et al., 2007; Juniam and Arthur, 2007; Juniam and Arthur, 2018).

Further studies of the area are pending and will be shared among the IODP 369 Expedition scientists and will be in publication shortly. Future studies of the area are already being carried out, such as more accurate age dating, construction of a biostratigraphic column, trace metal analysis, which is being done by Dr. Laurent Riquier's team, and grain size analysis done by Dr. Zhaokai Xu's team. OAE 1d is not identifiable at these locations with the data collected so far. To fully support or disprove this statement, a multi proxy using $\delta^{13}C_{org}$ and TOC investigation needs to be carried out (Scholle and Arthur, 1980, Jenykns, 2010: Scott et al., 2013; Bottini and Erba, 2018). The two Holes are not far apart at their current day positions but are classified slightly differently in Harry et al., (2020). The scholars classify Hole U1513C as located in the western Mentelle Basin and Hole U1516C in the central Mentelle Basin. The research in Harry et al., (2020) focuses on breakup events and subsidence history of the southwestern Australian margin, rather than on other aspects, such as paleoposition of the sites during OAE 1d or paleocurrents. This is another area that warrants further research in future studies.

REFERENCES

Altabet, M.A., and Francois, R., 1994, Sedimentary nitrogen isotopic ratio as a recorder for surface ocean nitrate utilization: Global Biogeochemical Cycles, v. 8, p. 103–116, doi: 10.1029/93gb03396.

Borissova, I., Bradshaw, B., Nicholson, C., Struckmeyer, H., and Payne, D., 2010, New exploration opportunities on the southwest Australian margin—deep-water frontier Mentelle Basin: The APPEA Journal, v. 50, p. 47, doi: 10.1071/aj09004.

Bottini, C., and Erba, E., 2018, Mid-Cretaceous paleoenvironmental changes in the western Tethys: Climate of the Past, v. 14, p. 1147–1163, doi: 10.5194/cp-14-1147-2018.

Brodie, C.R., Heaton, T.H.E., Leng, M.J., Kendrick, C.P., Casford, J.S.L., and Lloyd, J.M., 2011, Evidence for bias in measured $\delta^{15}N$ values of terrestrial and aquatic organic materials due to pre-analysis acid treatment methods: Rapid Communications in Mass Spectrometry, v. 25, p. 1089–1099, doi: 10.1002/rcm.4970.

Dill, H., 2020, A geological and mineralogical review of clay mineral deposits and phyllosilicate ore guides in Central Europe – A function of geodynamics and climate change: Ore Geology Reviews, v. 119, p. 103304, doi: 10.1016/j.oregeorev.2019.103304.

Giraud, F., Olivero, D., Baudin, F., Reboulet, S., Pittet, B., and Proux, O., 2003, Minor changes in surface-water fertility across the oceanic anoxic event 1d (latest Albian, SE France) evidenced by calcareous nannofossils: International Journal of Earth Sciences, v. 92, p. 267–284, doi: 10.1007/s00531-003-0319-x.

Harry, D.L., Tejada, M.L.G., Lee, E.Y., Wolfgring, E., Wainman, C.C., Brumsack, H.J., Schnetger, B., Kimura, J.I., Riquier, L., Borissova, I., Hobbs, R.W., Jiang, T., Li, Y.X., Maritati, A., et al., 2020, Evolution of the Southwest Australian Rifted Continental Margin During Breakup of East Gondwana: Results From International Ocean Discovery Program Expedition 369: Geochemistry, Geophysics, Geosystems, v. 21, doi: 10.1029/2020gc009144.

Hay, W.W., 2008, Evolving ideas about the Cretaceous climate and ocean circulation: Cretaceous Research, v. 29, p. 725–753, doi: 10.1016/j.cretres.2008.05.025.

Huber, B.T., Hobbs, R.W., Bogus, K.A., Batenburg, S.J., Brumsack, H.-J., Guerra, R.D.M., Edgar, K.M., Edvardsen, T., Garcia Tejada, M.I., Harry, D.L., Hasegawa, T., Haynes, S.J., Jiang, T., Jones, M.M., et al., 2019, Expedition 369 summary: Proceedings of the International Ocean Discovery Program, doi: 10.14379/iodp.proc.369.101.2019.

Huber, B.T., Hobbs, R.W., Bogus, K.A., and the Expedition 369 Scientists, 2018. Expedition 369 Preliminary Report: Australia Cretaceous Climate and Tectonics. International Ocean Discovery Program. https://doi.org/10.14379/iodp.pr.369.2018

Gallagher, S., Taylor, D., Apthorpe, M., Stilwell, J., Boreham, C., Holdgate, G., Wallace, M., and Quilty, P., 2005, Late Cretaceous dysoxia in a southern high latitude siliciclastic succession, the Otway Basin, southeastern Australia: Palaeogeography, Palaeoclimatology, Palaeoecology, v. 223, p. 317–348, doi: 10.1016/j.palaeo.2005.04.017.

Jenkyns, H.C., 2003, Evidence for rapid climate change in the Mesozoic–Palaeogene greenhouse world: Philosophical Transactions of the Royal Society of London. Series A: Mathematical, Physical and Engineering Sciences, v. 361, p. 1885–1916, doi: 10.1098/rsta.2003.1240.

Jenkyns, H.C., 2010, Geochemistry of oceanic anoxic events: Geochemistry, Geophysics, Geosystems, v. 11, doi: 10.1029/2009gc002788.

Jenkyns, H.C., 2018, Transient cooling episodes during Cretaceous Oceanic Anoxic Events with special reference to OAE 1a (Early Aptian): Philosophical Transactions of the Royal Society A: Mathematical, Physical and Engineering Sciences, v. 376, p. 20170073, doi: 10.1098/rsta.2017.0073.

Jenkyns, H.C., Gröcke, D.R., and Hesselbo, S.P., 2001, Nitrogen isotope evidence for water mass denitrification during the Early Toarcian (Jurassic) oceanic anoxic event: Paleoceanography, v. 16, p. 593–603, doi: 10.1029/2000pa000558

Jenkyns, H.C., Matthews, A., Tsikos, H., and Erel, Y., 2007, Nitrate reduction, sulfate reduction, and sedimentary iron isotope evolution during the Cenomanian-Turonian oceanic anoxic event: Paleoceanography, v. 22, doi: 10.1029/2006pa001355.

Junium, C.K., and Arthur, M.A., 2007, Nitrogen cycling during the Cretaceous, Cenomanian-Turonian Oceanic Anoxic Event II: Geochemistry, Geophysics, Geosystems, v. 8, doi: 10.1029/2006gc001328.

Junium, C.K., Dickson, A.J., and Uveges, B.T., 2018, Perturbation to the nitrogen cycle during rapid Early Eocene global warming: Nature Communications, v. 9, doi: 10.1038/s41467-018-05486-w.

Karl, D., and Michaels, A., 2001, Nitrogen Cycle: Encyclopedia of Ocean Sciences, p. 1876–1884, doi: 10.1006/rwos.2001.0275.

Leckie, R.M., Bralower, T.J., and Cashman, R., 2002, Oceanic anoxic events and plankton evolution: Biotic response to tectonic forcing during the mid-Cretaceous: Paleoceanography, v. 17, doi: 10.1029/2001pa000623.

Lee, E.Y., Wolfgring, E., Tejada, M.L.G., Harry, D.L., Wainman, C.C., Chun, S.S., Schnetger, B., Brumsack, H.-J., Maritati, A., Martinez, M., Richter, C., Li, Y.-X., Riquier, L., Macleod, K.G., et al., 2020, Early Cretaceous subsidence of the Naturaliste Plateau defined by a new record of volcaniclastic-rich sequence at IODP Site U1513: Gondwana Research, v. 82, p. 1–11, doi: 10.1016/j.gr.2019.12.007.

Ludvigson G.A., Gonzalez L.A., Ufnar D.F., Witzke B.J., Brenner R.L., 2002, Methane fluxes from mid-Cretaceous wetland soils: Insights gained from carbon and oxygen isotopic studies of sphaerosiderites in paleosols. Geological Society of America, Abstracts with Programs, 34 (6), p. 212

Maritati, A., Halpin, J.A., Whittaker, J.M., Daczko, N.R., and Wainman, C.C., 2021, Provenance of Upper Jurassic–Lower Cretaceous strata in the Mentelle Basin, southwestern Australia, reveals a trans-Gondwanan fluvial pathway: Gondwana Research, v. 93, p. 128–141, doi: 10.1016/j.gr.2020.12.032.

Meyer, K.M., and Kump, L.R., 2008, Oceanic Euxinia in Earth History: Causes and Consequences: Annual Review of Earth and Planetary Sciences, v. 36, p. 251–288, doi: 10.1146/annurev.earth.36.031207.124256.

Ohkouchi, N., Kashiyama, Y., Kuroda, J., Ogawa, N.O., and Kitazato, H., 2006, The importance of diazotrophic cyanobacteria as primary producers during Cretaceous Oceanic Anoxic Event 2: Biogeosciences, v. 3, p. 467–478, doi: 10.5194/bg-3-467-2006.

Petrizzo, M.R., Huber, B.T., Wilson, P.A., and Macleod, K.G., 2008, Late Albian paleoceanography of the western subtropical North Atlantic: Paleoceanography, v. 23, doi: 10.1029/2007pa001517.

Quan, T.M., Adigwe, E.N., Riedinger, N., and Puckette, J., October 2013b, Evaluating nitrogen isotopes as proxies for depositional environmental conditions in shales: Comparing Caney and Woodford Shales in the Arkoma Basin, Oklahoma: Chemical Geology, v. 360-361, p. 231–240, doi: 10.1016/j.chemgeo.2013.10.017

Quan, T.M., Wright, J.D., and Falkowski, P.G., March 2013a, Co-variation of nitrogen isotopes and redox states through glacial–interglacial cycles in the Black Sea: Geochimica et Cosmochimica Acta, v. 112, p. 305–320, doi: 10.1016/j.gca.2013.02.029.

Rivera, K.T., Puckette, J., and Quan, T.M., 2015, Evaluation of redox versus thermal maturity controls on $\delta^{15}N$ in organic rich shales: A case study of the Woodford Shale, Anadarko Basin, Oklahoma, USA: Organic Geochemistry, v. 83-84, p. 127–139, doi: 10.1016/j.orggeochem.2015.03.005.

Tyson, R.V., and Pearson, T.H., 1991, Modern and ancient continental shelf anoxia: an overview: Geological Society, London, Special Publications, v. 58, p. 1–24, doi: 10.1144/gsl.sp.1991.058.01.01.

Rau, G.H., Arthur, M.A., and Dean, W.E., 1987, 15N/14N variations in Cretaceous Atlantic sedimentary sequences: implication for past changes in marine nitrogen biogeochemistry: Earth and Planetary Science Letters, v. 82, p. 269–279, doi: 10.1016/0012-821x(87)90201-9.

Schlanger, S. O., and Jenkyns, H. C., 1976, Cretaceous Oceanic Anoxic Events: Causes and Consequences: Geologie En Mijnbouw, v. 55, pp. 179–184.

Scholle, P. A., and M. A. Arthur, 1980, Carbon isotope fluctuations in Cretaceous pelagic limestones: Potential stratigraphic and petroleum exploration tool, AAPG Bull., 64, 67–87

Sigman, D., and Casciotti, K., 2001, Nitrogen Isotopes in the Ocean: Encyclopedia of Ocean Sciences, p. 1884–1894, doi: 10.1006/rwos.2001.0172.

Scott, R., Formolo, M., Rush, N., Owens, J.D., and Oboh-Ikuenobe, F., 2013, Upper Albian OAE 1d event in the Chihuahua Trough, New Mexico, U.S.A.: Cretaceous Research, v. 46, p. 136–150, doi: 10.1016/j.cretres.2013.08.011.

Walther, J.V., 2009, Essentials of geochemistry: Sudbury, MA, Jones and Bartlett Publishers.

Wilson, P.A., and Norris, R.D., 2001, Warm tropical ocean surface and global anoxia during the mid-Cretaceous period: Nature, v. 412, p. 425–429, doi: 10.1038/35086553.

APPENDICES

Table A1. $\delta^{15}N_{acidified}$ results for U1513C. Intervals with underlined text denote the suspected Ocean Anoxic Event 1d interval (from personal communication with Dr. Macleod and Dr. Hasegawa, April 2019). The depth is denoted as core depth below seafloor (CSF-A), measured in meters, which is equivalent to meters below seafloor (Huber et al., 2019).

Sample ID	$\delta^{15}N_{acidified}$	CSF-A (m)
1513-24R-6w - 38/40	-0.6	294.89
151325R-1w - 15/17	0.6	296.75
1513-25R-1w - 69/71	0.4	297.29
1513-25R-1w - 134/136	0.8	297.94
1513-25R-2w - 32/34	0.5	298.43
1513-25R-2w - 87/89	0.6	298.98
1513-25R-2w - 134/136	0.8	299.45
1513-25R-3w - 45/47	1.6	300.06
1513-25R-3w - 82/84	0.6	300.43
1513-25R-3w - 104/106	0.4	300.64
1513-25R-3w - 139/141	0.4	300.99
1513-25R-4w - 35/37	0.8	301.46
1513-25R-4w - 65/67	0.8	301.77
1513-25R-4w - 82/84	0.7	301.93
1513-25R-5w - 54/56	1.1	302.67
1513-25R-5w - 72/74	0.4	302.85
1513-25R-5w - 87/89	0.9	303
1513-25R-6w - 3/5	1.2	303.17
1513-25R-6w - 14/16	1.7	303.27
1513-25R-6w - 23/25	-0.5	303.36
1513-25R-6w - 30/32	0.2	303.43
1513-25R-7w - 39/41	-0.1	303.53
1513-25R-6w - 52/54	-0.2	303.65
1513-26R-6w - 60/62	0.06	303.73
1513-25R-6w -72/74	0.04	303.85

1513-25R-6w - 89/91	-0.5	304.02
1513-25R-7w - 4/6	-0.2	304.14
1513-25R-7w - 46/48	-0.6	304.56
1513-25R-ccw - 2/4	0.08	304.63
1513-25R-ccw - 7/9	-0.8	304.68
1513-25R-ccw - 11/13	-0.08	304.72
1513-25R-ccw - 17/19	0.6	304.78
1513-26R-1w - 10/12	-0.07	306.3
1513-26R-1w - 14/16	-0.4	306.34
1513-26R-1w - 25/27	-0.4	306.45
1513-26R-1w - 30/32	-0.9	306.5
1513-26R-1w - 33/35	-0.4	306.53
1513-26R-1w - 34/36	0.2	306.58
1513-26R-1w - 38/40	-0.1	306.63
1513-26R-1w - 43/45	0.007	306.68
1513-26R-1w - 48/50	0.5	306.73
1513-26R-1w - 53/55	1.2	306.82
1513-26R-1w - 62/64	0.8	306.87
1513-26R-1w - 67/69	0.1	307.09
1513-26R-1w - 89/91	0.2	307.14
1513-26R-1w - 94/96	-1.3	307.18
1513-26R-1w - 98/100	-1.6	307.36
1513-26R-1w - 116/118	-1.0	307.55
1513-26R-2w - 4/6	-0.9	307.61
1513-26R-2w - 10/12	-0.9	307.65
1513-26R-2w - 14/16	-0.005	307.7
1513-26R-2w - 19/21	-0.1	307.75
1513-26R-2w - 24/26	-0.2	307.8
1513-26R-2w - 29/31	-0.9	307.85
1513-26R-2w - 45/47	-0.4	307.96
1513-26R-2w -49/51	-0.8	308
1513-26R-2w - 56/58	-1.0	308.07
1513-26R-2w - 61/63	0.4	308.12
1513-26R-2w - 64/66	-0.2	308.15
1513-26R-2w - 69/71	-0.5	308.2
1513-26R-2w - 77/79	-0.5	308.28
1513-26R-2w - 81/83	-0.3	308.32
1513-26R-2w - 86/88	-0.2	308.37

1513-26R-2w - 91/93	-0.1	308.42
1513-26R-2w - 95/97	0.4	308.46
1513-26R-2w - 106/108	0.5	308.57
1513-26R-2w - 121/123	2.1	308.72
1513-26R-2w - 137/139	2.2	308.88
1513-26R-3w - 30/32	0.9	309.31
1513-26R-3w - 47/49	1.5	309.48
1513-26R-3w - 82/84	1.1	309.83
1513-26R-4w - 8/10	0.4	310.48
1513-26R-4w - 20/22	0.1	310.61
1513-26R-ccw - 13/15	-0.9	311.03
1513-27R-1w - 5/7	-0.02	315.85
1513-27R-1w - 13/15	-0.04	315.93
1513-27R-1w - 18/20	0.8	315.98
1513-27R-1w - 23/25	-0.2	316.03
1513-27R-1w - 28/30	0.08	316.08
1513-27R-1w - 33/35	-0.6	316.13
1513-27R-1w - 37/39	-0.4	316.17
1513-27R-1w - 43/45	0.6	316.23
1513-27R-1w - 48/50	1.5	316.28
1513-27R-1w - 53/55	-0.09	316.33
1513-27R-1w - 58/60	-0.08	316.38
1513-27R-1w - 62/64	0.4	316.42
1513-27R-1w - 72/74	1.1	316.52
1513-27R-1w - 77/79	0.9	316.57
1513-27R-1w - 84/86	-0.2	316.64
1513-27R-1w - 89/91	-0.7	316.69
1513-27R-1w - 95/97	0.2	316.75
1513-27R-1w - 100/102	-0.02	316.8
1513-27R-1w - 103/105	-0.3	316.83
1513-27R-2w - 3/5	-0.1	316.89
1513-27R-2w - 7/9	-0.05	316.94
1513-27R-2w - 11/13	0.7	316.98
1513-27R-2w - 14/16	-0.1	317.01
1513-27R-2w - 22/24	-0.03	317.09
1513-27R-2w - 27/29	-	317.14
1513-27R-2w - 34/36	-0.4	317.21
1513-27R-2w - 40/42	-0.2	317.27

1513-27R-2w - 48/50	-0.4	317.35
1513-27R-2w - 53/55	-0.04	317.4
1513-27R-2w - 58/60	0.07	317.45
1513-27R-2w - 63/65	0.02	317.5
1513-27R-2w - 68/70	0.1	317.55
1513-27R-2w - 71/73	0.4	317.58
1513-27R-2w - 75/77	0.7	317.62
1513-27R-2w - 82/84	0.8	317.69
1513-27R-2w - 88/90	0.2	317.75
1513-27R-2w - 107/109	0.6	317.94
1513-27R-2w - 112/114	0.2	317.99
1513-27R-2w - 116/118	-	318.03
1513-27R-2w - 121/123	-0.03	318.08
1513-27R-2w - 116/118	-1.0	318.13
1513-27R-2w - 126/128	-0.3	318.17
1513-27R-2w - 130/132	-0.1	318.44
1513-27R-3w - 7/9	-0.6	318.62
1513-27R-3w - 25/27	-0.5	318.92
1513-27R-3w - 55/57	0.6	319.57
1513-27R-3w - 120/122	-0.09	320.03
1513-27R-4w - 16/18	-0.5	320.42
1513-27R-4w - 57/59	-0.3	320.51
1513-27R-4w - 64/66	0.06	320.66
1513-27R-ccw - 7/9	-0.2	325.5
1513-28R-1w - 10/12	-0.1	325.95
1513-28R-1w - 55/57	0.5	326.49
1513-28R-1w - 109/111	-0.08	327.05
1513-28R-2w - 15/17	-0.2	327.61
1513-28R-2w - 71/73	1.2	328.21
1513-28R-2w - 131/133	0.5	328.81
1513-28R-3w - 40/42	0.2	329.36
1513-28R-3w - 95/97	-0.3	329.86
1513-28R-3w - 145/147	-0.4	330.32
1513-28R-4w - 40/42	0.2	330.95
1513-28R-4w - 103/105	-0.2	331.47
1513-28R-5w - 6/8	0.5	332.05
1513-28R- 5w - 64/66	-0.1	332.63
1513-28R-5w - 112/124	-0.3	333.16

1513-28R-6w - 25/27	0.2	333.7
1513-28R-ccw - 10/12	-0.3	334.7

Table A2. $\delta^{15}N_{acidified}$ results for U1516C. Intervals with underlined text denote the suspected Ocean Anoxic Event 1d interval (from personal correspondence). The depth is denoted as core depth below seafloor (CSF-A), measured in meters, which is equivalent to meters below seafloor (Huber et al., 2019).

Sample ID	$\delta^{15}N_{acidified}$	**Top depth CSF-A (m)**
1516-38R-1w - 42/44	-0.3	503.64
1516-38R-1w - 100/102	-0.3	504.22
1516-38R-2w - 10/12	-0.3	504.66
1516-38R-2w - 60/62	-0.7	505.16
1516-38R-3w - 26/28	-0.07	505.46
1516-38R-3w - 45/47	-0.04	505.65
1516-38R-3w - 65/67	0.2	505.85
1516-38R-3w - 84/86	0.2	506.04
1516-38R-3w - 105/107	0.2	506.25
1516-38R-4w - 16/18	0.7	506.55
1516-38R-4w - 35/37	0.4	506.74
1516-38R-4w - 52/54	0.6	506.91
1516-38R-4w - 79/81	-0.2	507.18
1516-38R-4w - 102/104	-0.3	507.41
1516-38R-4w - 123/125	-0.1	507.62
1516-38R-5w - 5/7	-0.3	507.79
1516-38R-5w - 18/20	0.4	507.9
1516-38R-5w - 43/45	0.3	508.15
1516-38R-5w - 55/57	-0.3	508.27
1516-38R-5w - 63/65	-1.02	508.35
1516-38R-5w - 73/75	-0.8	508.45
1516-38R-5w - 82/84	-0.9	508.54
1516-38R-5w - 92/94	-0.4	508.64
1516-38R-6w - 3/5	-1.1	508.77
1516-38R-6w - 15/17	-0.3	508.89
1516-38R-6w - 24/26	0.05	508.98
1516-38R-6w - 32/34	*-0.2*	*509.06*
1516-38R-6w - 43/45	*-0.4*	*509.17*

1516-38R-6w - 46/48	*-0.3*	*509.2*
1516-38R-6w - 55/57	*-0.4*	*509.29*
1516-38R-6w - 60/62	*-0.5*	*509.34*
1516-38R-6w - 65/67	*-0.2*	*509.39*
1516-38R-6w - 70/72	*0.2*	*509.44*
1516-38R-ccw - 6/8	*-0.04*	*509.54*
1516-38R-ccw - 13/15	*-0.2*	*509.61*
1516-39R-1w - 4/6	*-0.7*	*512.84*
1516-39R-1w - 10/12	*-0.9*	*512.9*
1516-39R-1w - 14/16	*0.1*	*512.94*
1516-39R-1w - 22/24	*-0.6*	*513.02*
1516-39R-1w - 24/26	*-1.1*	*513.04*
1516-39R-1w - 30/32	*-0.9*	*513.1*
1516-39R-1w - 34/36	*-0.9*	*513.14*
1516-39R-1w - 43/45	*-0.6*	*513.23*
1516-39R-1w - 45/47	*0.3*	*513.25*
1516-39R-1w - 50/52	*0.2*	*513.3*
1516-39R-1w - 55/57	*-0.7*	*513.35*
1516-39R-1w - 60/62	*-0.4*	*513.4*
1516-39R-1w - 65/67	*-0.2*	*513.45*
1516-39R-1w - 71/73	*-0.4*	*513.51*
1516-39R-1w - 76/78	*0.4*	*513.56*
1516-39R-1w - 83/85	*-0.4*	*513.63*
1516-39R-2w - 2/4	*-0.3*	*513.76*
1516-39R-2w - 7/9	*-0.6*	*513.81*
1516-39R-2w - 13/15	*-0.6*	*513.87*
1516-39R-2w - 16/18	*-0.6*	*513.9*
1516-39R-2w - 23/25	*0.2*	*513.97*
1516-39R-2w - 27/29	*-0.8*	*514.01*
1516-39R-2w - 31/33	*-0.7*	*514.05*
1516-39R-2w - 37/39	*-0.6*	*514.11*
1516-39R-2w - 43/45	*-0.7*	*514.17*
1516-39R-2w - 48/50	*-0.6*	*514.22*

1516-39R-2w p 53/55	*-1.2*	*514.27*
1516-39R-2w - 60/62	*-0.5*	*514.34*
1516-39R-2w - 68/70	*-0.7*	*514.42*
1516-39R-2w - 73/75	*-1.1*	*514.47*
1516-39R-ccw - 3/5	-0.7	514.58
1516-40R-1w - 2/4	-1.05	522.42
1516-40R-1w - 36/38	-0.3	522.76
1516-40R-1w - 52/54	-0.04	522.92
1516-40R-1w - 73/75	0.2	523.13
1516-40R-1w - 93/95	0.1	523.33
1516-40R-1w - 141/143	0.2	523.81
1516-40R-2w - 45/47	-0.2	524.36
1516-40R-2w - 94/96	-0.4	524.85
1516-40R-2w - 145/147	0.4	525.36
1516-40R-3w -b43/45	-0.03	525.87
1516-40R-3w - 94/96	-0.006	526.38
1516-40R-4w - 23/25	-0.2	526.85
1516-40R-4w - 75/77	-0.6	527.37
1516-40R-4w - 113/115	0.5	527.75

Table A3. Standard Deviations of Standards for all samples

		USGS-40
		0.08
		0.09
		0.06
		0.2
		0.2
		0.2
		0.2
		0.1
		0.4
		0.1
MIN		0.06
MAX		0.4

Table A4. Standard Deviations of sediment duplicates for all samples

	DUPLICATE STANDARD DEVIATIONS
	0.7
	0.5
	0.04
	0.3
	0.6
	0.2
	0.2
	0.06
	0.04
	0.06
	0.2
	0.6
	0.1
	0.3
	0.2
	0.02
	0.03
MIN	0.02
MAX	0.7

VITA

Hannah Jessica Ghotbi

Candidate for the Degree of

Master of Science

Thesis: STABLE ISOTOPE INVESTIGATION OF THE PRESENCE OF OCEAN ANOXIC EVENT 1D IN MENTELLE BASIN

Major Field: GEOLOGY

Biographical:

Education: The University of Texas at Dallas

Completed the requirements for the Master of Science in Geology at Oklahoma State University, Stillwater, Oklahoma in July 2021.

Completed the requirements for the Bachelor of Science in Geosciences at The University of Texas at Dallas, Richardson, Texas in 2017.

Experience:
N/A

Professional Memberships:
American Institute of Professional Geologists (AIPG)
Association for Women in Geosciences (AWG)